iScience

CellPress

Article

Aryl Hydrocarbon Receptor Promotes Liver Polyploidization and Inhibits PI3K, ERK, and Wnt/β-Catenin Signaling

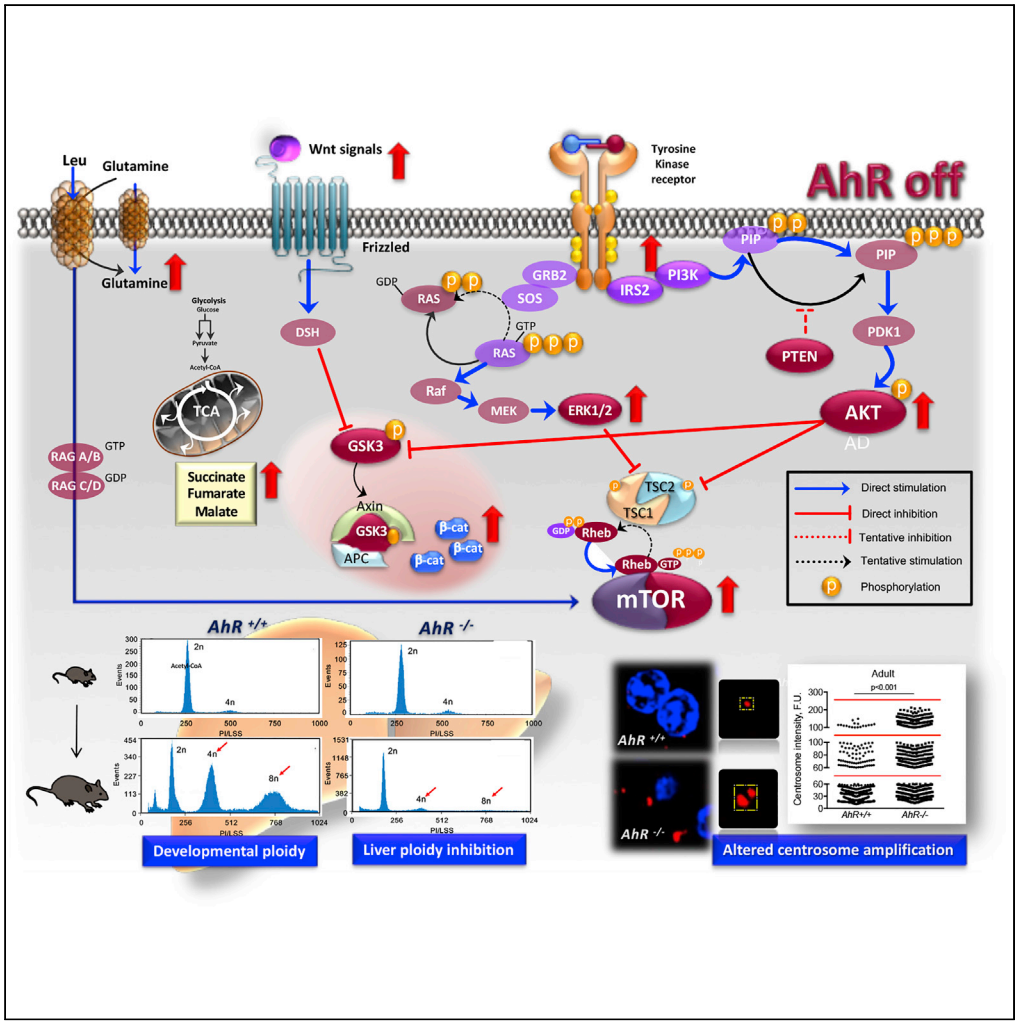

Nuria Moreno-Marín, Jaime M. Merino, Alberto Alvarez-Barrientos, ..., Alberto Muñoz, Frank J. Gonzalez, Pedro M. Fernández-Salguero

pmfersal@unex.es

HIGHLIGHTS

AhR is required for liver polyploidization during preweaning-to-adult transition

INS-R/PI3K/AKT, ERK, Wnt/β-Cat and mTOR are downregulated during liver polyploidization

Reduced polyploidy relates with enhanced mitochondrial metabolism in AhR-null liver

Understanding how AhR modulates polyploidy may provide strategies against cancer

Moreno-Marín et al., iScience 4, 44–63
June 29, 2018
https://doi.org/10.1016/j.isci.2018.05.006

iScience

CellPress

Article

Aryl Hydrocarbon Receptor Promotes Liver Polyploidization and Inhibits PI3K, ERK, and Wnt/β-Catenin Signaling

Nuria Moreno-Marín,[1] Jaime M. Merino,[1] Alberto Alvarez-Barrientos,[2] Daxeshkumar P. Patel,[3] Shogo Takahashi,[3] José M. González-Sancho,[4] Pablo Gandolfo,[5] Rosa M. Rios,[5] Alberto Muñoz,[4] Frank J. Gonzalez,[3] and Pedro M. Fernández-Salguero[1,6,*]

SUMMARY

Aryl hydrocarbon receptor (AhR) deficiency alters tissue homeostasis. However, how AhR regulates organ maturation and differentiation remains mostly unknown. Liver differentiation entails a polyploidization process fundamental for cell growth, metabolism, and stress responses. Here, we report that AhR regulates polyploidization during the preweaning-to-adult mouse liver maturation. Preweaning AhR-null (*AhR−/−*) livers had smaller hepatocytes, hypercellularity, altered cell cycle regulation, and enhanced proliferation. Those phenotypes persisted in adult *AhR−/−* mice and correlated with compromised polyploidy, predominance of diploid hepatocytes, and enlarged centrosomes. Phosphatidylinositol-3-phosphate kinase (PI3K), extracellular signal-regulated kinase (ERK), and Wnt/β-catenin signaling remained upregulated from preweaning to adult AhR-null liver, likely increasing mammalian target of rapamycin (mTOR) activation. Metabolomics revealed the deregulation of mitochondrial oxidative phosphorylation intermediates succinate and fumarate in *AhR−/−* liver. Consistently, PI3K, ERK, and Wnt/β-catenin inhibition partially rescued polyploidy in *AhR−/−* mice. Thus, AhR may integrate survival, proliferation, and metabolism for liver polyploidization. Since tumor cells tend to be polyploid, AhR modulation could have therapeutic value in the liver.

INTRODUCTION

Most eukaryotic cells have a diploid cell cycle in which chromosomes are replicated only once during each cell division to generate two identical 2n daughter cells. Nevertheless, certain organisms can undergo successive rounds of genome duplication in the absence of cytokinesis to acquire a polyploid status that can involve the whole organism or just specific tissues and organs (Edgar et al., 2014; Fox and Duronio, 2013; Schoenfelder and Fox, 2015). Among mammals, including humans, polyploidy is particularly relevant in the liver hepatocytes, megakaryocytes, and placental giant trophoblast cells, although it also takes place in the heart and muscle (Gentric et al., 2012; Hannibal et al., 2014). In the liver, the percentage of polyploid hepatocytes ranges from 80% to 90% in rats, to 30% in humans, and to close to 50% in mice (Celton-Morizur et al., 2010; Duncan et al., 2010). Polyploidy does not seem to be a uniform phenomenon, and usually aneuploid cells with altered number of chromosomes co-exist with cells having ≥2n DNA content (Schoenfelder and Fox, 2015). Several mechanisms have been proposed to explain physiological polyploidy, including failure to complete cytokinesis after mitosis of diploid hepatocytes (Guidotti et al., 2003), cell fusion of placental cells, or endomitosis in megakaryocytes (Ullah et al., 2009; Zielke et al., 2013). Recent reports have suggested that polyploidization may not be an irreversible process since mouse hepatocytes with one-half chromosomal content can be obtained from polyploid liver cells by artificial cell fusion (Duncan et al., 2009; Wang et al., 2003). Such phenomena would then generate mixed cell populations with dissimilar number of chromosomes by a process named ploidy conveyor (Duncan et al., 2010).

Physiological polyploidy takes place in the mouse liver right after the transition from preweaning (approximately 3 weeks after birth) to adulthood (Marques et al., 2008; Pandit et al., 2012, 2013). During this period, immature hepatoblasts start to differentiate into mature hepatocytes concomitantly with a reduction in their proliferative ability (Germain et al., 1988; Shiojiri et al., 1991). From a functional perspective, polyploidy induces a terminal differentiated phenotype that increases cell size, amplifies gene expression, helps tissue organization, and modifies hepatic metabolism (Schoenfelder and Fox, 2015; Zielke et al., 2013). In fact, transcriptomic studies have revealed that larger polyploid hepatocytes switch their

[1]Departamento de Bioquímica y Biología Molecular, Facultad de Ciencias, Universidad de Extremadura, Badajoz, Badajoz 06071, Spain

[2]Servicio de Técnicas Aplicadas a las Biociencias (STAB), Universidad de Extremadura, Badajoz, Badajoz 06071, Spain

[3]Laboratory of Metabolism, Center for Cancer Research, National Cancer Institute, National Institutes of Health, Bethesda, MD 20892, USA

[4]Instituto de Investigaciones Biomédicas "Alberto Sols", Consejo Superior de Investigaciones Científicas – Universidad Autónoma de Madrid, and CIBER de Cáncer (CIBERONC), Instituto de Salud Carlos III, Madrid 28029, Spain

[5]Cell Signaling Department, CABIMER-CSIC, Sevilla 41092, Spain

[6]Lead Contact

*Correspondence: pmfersal@unex.es

https://doi.org/10.1016/j.isci.2018.05.006

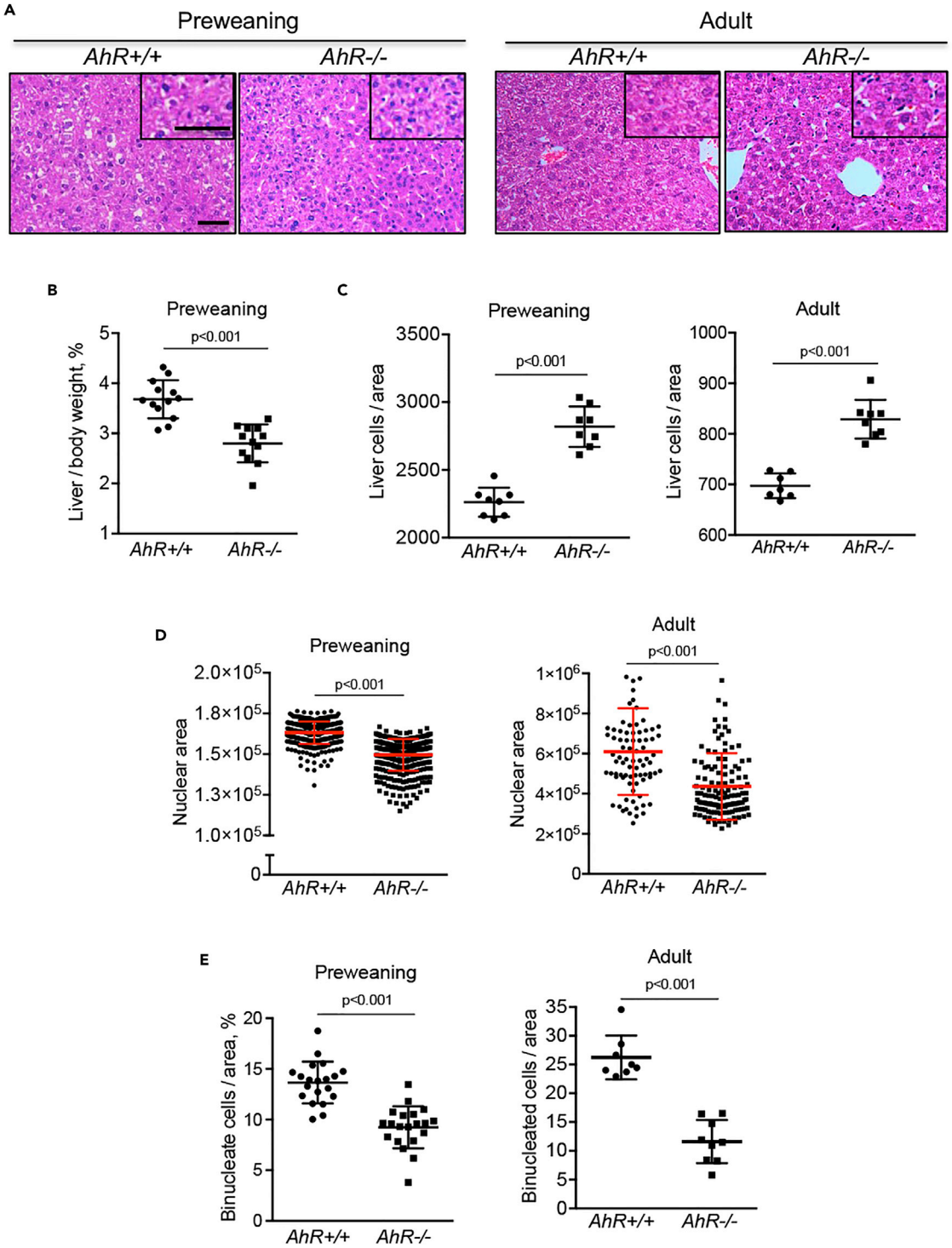

Figure 1. AhR-Null Liver has Hypercellularity, Increased Nuclear Size, and Reduced Number of Binucleated Hepatocytes

(A) Livers were collected from preweaning and adult *AhR+/+* and *AhR−/−* mice, fixed, embedded in paraffin, sectioned, and stained with hematoxylin and eosin (H&E).

(B) Relative liver weight was obtained in preweaning mice relative to the total body weight of each animal.

(C) Liver cellularity was quantified in tissue sections obtained from preweaning and adult AhR mice of each genotype.

(D) Nuclear area of hepatocytes was determined in *AhR+/+* and *AhR−/−* liver sections from preweaning and adult mice after staining with DAPI. ImageJ software was used.

Figure 1. *Continued*

(E) Binucleated cells in preweaning and adult *AhR+/+* and *AhR−/−* livers were quantified by confocal fluorescence microscopy using DAPI-stained sections. Six mice for each developmental time and genotype and three technical replicates were analyzed.

Data are shown as mean ± SD. Scale bar, 50 μm; scale bar in inset, 50 μm. Nuclear area is represented as the integrated density (IntDen) measured by the ImageJ software in micrographs taken at the same magnification and resolution. SD, standard deviation.

metabolism from mitochondrial oxidative phosphorylation to glycolysis to adapt to metabolic stresses, although some controversy exists on the relative contribution of ploidy versus cell size in their metabolic reprogramming (Miettinen et al., 2014). The liver is exposed to the deleterious effects of endo- and xenobiotics and, as such, has the remarkable property to regenerate upon injury (Taub, 2004). Polyploid hepatocytes can therefore trigger a response against toxic compounds by entering mitosis and generating proliferative hepatocytes that will reconstitute the damaged parenchyma (Duncan et al., 2012). Importantly, several human cancers seem to contain polyploid cells that can re-enter cell cycle acquiring Warburg-like glycolytic metabolism and contributing to tumor growth (Davoli and de Lange, 2011; Ganem et al., 2007; Zack et al., 2013).

The aryl hydrocarbon/dioxin receptor (AhR) has many different physiological and homeostatic functions some of which are now beginning to emerge. Mouse models have shown that complete AhR depletion alters the development and function of several organs, including the liver, heart, skin, and immune system (Esser and Rannug, 2015; Mulero-Navarro and Fernandez-Salguero, 2016; Pohjanvirta, 2012; Puga et al., 2009; Schmidt and Bradfield, 1996). Despite early studies showing that adult AhR-null mice (*AhR−/−*) have smaller livers (Fernandez-Salguero et al., 1995, 1997; Schmidt et al., 1996) with embryo-derived intrahepatic portosystemic shunt (Lahvis et al., 2000; Schmidt et al., 1996), there are no studies exploring how AhR affects liver maturation and differentiation during the critical postnatal to adulthood developmental window.

In this work, we have investigated whether AhR is needed for the diploid-to-polyploid conversion that takes place during the transition from an immature to an adult liver. AhR deficiency severely compromised the generation of polyploid hepatocytes and maintained a more proliferative liver under physiological conditions. Persistent upregulation of signaling pathways controlling survival, proliferation, and metabolism in adult AhR-null liver likely compromised polyploidization and favored a diploid and undifferentiated phenotype. Such attributes could greatly influence the regenerative competence of the *AhR−/−* liver in the short term as well as its increased ability to develop hepatocarcinomas upon carcinogen exposure in the long term (Moreno-Marín et al., 2017). Thus, AhR is a relevant component of a complex signaling network controlling physiological liver polyploidy and differentiation. Selective AhR modulators may be useful to regulate ploidy-related liver responses such as those required for regeneration after toxic damage or surgical intervention or for inhibition of tumor progression.

RESULTS

AhR Deficiency Increases Liver Cellularity and Proliferation and Impairs Adult Polyploidy

Early reports showed that AhR-null mice (*AhR−/−*) have developmental hepatic alterations, including a reduced organ size (Fernandez-Salguero et al., 1995; Schmidt et al., 1996). In this work, we have used mice around the time of weaning (25 days of age, hereafter preweaning) and adult mice (9–10 weeks of age) having or lacking AhR expression. Histological examination of liver sections from preweaning and adult *AhR−/−* mice suggested an increase in cellularity with respect to age-matched *AhR+/+* mice (Figure 1A), despite the smaller liver size of AhR-null preweaning mice (Figure 1B). Adult *AhR−/−* mice also have a significant reduction in liver size and weight as previously reported (Fernandez-Salguero et al., 1995; Schmidt et al., 1996). This *de visu* observation was confirmed by cell counting and, indeed, *AhR−/−* livers had significantly higher numbers of hepatocytes than *AhR+/+* livers at preweaning and adult age (Figure 1C). Cellularity in adults was reduced with respect to preweaning livers regardless of mice genotype, possibly because of a normal developmental process that decreased cell proliferation and increased cell growth (Figure 1C). Accordingly, the average nuclear area of 4′,6-diamidino-2-phenylindole (DAPI)-stained *AhR−/−* hepatocytes was significantly smaller in both preweaning and adult livers (Figure 1D). In addition, the nuclei of preweaning hepatocytes were smaller than those of adult mice, irrespective of AhR expression (Figure 1D). Liver maturation involves several important cytological changes, including the appearance of binucleated and mononucleated polyploid hepatocytes (Gerlyng et al., 1993; Schoenfelder and Fox, 2015; Zielke et al., 2013). Interestingly, confocal fluorescence microscopy of

DAPI-stained liver sections revealed that whereas binucleated hepatocytes accounted for 25%–30% of liver cells in adult *AhR+/+* mice, they represented only about 10% of liver cells in aged-matched *AhR−/−* mice (Figure 1E). Binucleated hepatocytes were less abundant in preweaning mice and, in particular, in those lacking AhR expression (Figure 1E).

Altogether, these results suggested that lack of AhR could compromise physiological control of hepatocyte proliferation and the preweaning-to-adult transition in mouse liver. We then decided to analyze if the AhR-null phenotype could involve altered polyploidization since an increase in ploidy reduces proliferation and induces differentiation in the liver (Davoli and de Lange, 2011; Gentric and Desdouets, 2014; Ullah et al., 2009). Flow cytometry analysis of the DNA content of primary hepatocytes isolated from preweaning mice revealed that most cells were diploid (2c) in both *AhR+/+* and *AhR−/−* livers and that the amount of tetraploid (4c) and octaploid (8c) cells was minimal (Figures 2A, 2C, and S1). By contrast, adult *AhR+/+* livers became significantly enriched in 4c and 8c hepatocytes, whereas such enrichment was not found in *AhR−/−* hepatocytes, which remained mostly diploid (Figures 2B and 2D). A marked asymmetry in polyploidy was therefore observed between adult *AhR+/+* and *AhR−/−* livers (Figure 2E) that did not appear to be due to a significant level of endogenous apoptotic cell death (Figure 2F). Therefore, AhR controls normal liver architecture and cellularity and the nuclear content and ploidy of hepatocytes. Since polyploidization is related to liver differentiation, we next examined changes in albumin levels in preweaning and adult mice. Indeed, albumin messenger RNA (mRNA) (Figure 2G) and protein (Figure 2H) levels were significantly downregulated in *AhR−/−* livers at either developmental stage, suggesting that AhR expression is needed for physiological liver maturation.

AhR is known to regulate cell cycle progression by interacting with retinoblastoma protein (RB) and blocking E2F-dependent transcription of target genes such as Cyclin E (Gao et al., 2016; Mitchell et al., 2006; Pohjanvirta, 2012; Puga et al., 2002). AhR activation by TCDD (2,3,7,8-tetrachlorodibenzo-p-dioxin) also increases tumor suppressor $p27^{Kip1}$, which, in turn, inactivates Cyclin E (Kolluri et al., 1999; Siu et al., 2012). We then decided to analyze cell proliferation in mice liver *in vivo*. Ki67 staining of preweaning livers revealed high rates of cell proliferation in both genotypes, the number of proliferating cells being much higher in the absence of AhR than in control mice (Figure 3A). For adults, multiphoton confocal microscopy was used on tissue sections stained for the proliferating cell nuclear antigen (PCNA) because of the low rates of cell proliferation usually present in the matured liver. Although cell proliferation was markedly reduced with aging, *AhR−/−* livers still had more proliferative cells than *AhR+/+* livers (Figure 3A). Such increased proliferative potential of *AhR−/−* hepatocytes was associated with a higher number of cells passing through the G0/G1 (2c) and G2/M (4c) phases of the cell cycle, as determined by flow cytometry examination of freshly isolated primary hepatocytes (Figure 3B). Surprisingly, however, cell cycle regulators Cyclin B1 (G2/M) and Cyclin E (G1/S) were downregulated in liver from preweaning *AhR−/−* mice when compared with *AhR+/+* mice (Figures 3C and 3D). An opposite pattern of expression was observed in adult mice because both Cyclin B1 and Cyclin E were upregulated in AhR-null livers (Figures 3C and 3D). In addition, the expression of cyclin-dependent kinase inhibitory protein $p27^{Kip1}$ was markedly reduced in preweaning and adult *AhR−/−* livers (Figure 3E). No significant differences in Cyclin D1 (G1/S) were found between *AhR+/+* and *AhR−/−* livers at any developmental stage (not shown). These results suggest that high Cyclin B1 and Cyclin E expression, in parallel to reduced $p27^{Kip1}$ levels, could maintain proliferation and inhibit polyploidy in *AhR−/−* liver, in agreement with the role of Cip/Kip proteins in promoting differentiation and polyploidy in mammalian cells (Ullah et al., 2009). We next determined if the preweaning-to-adult transition involved changes in AhR expression. Immunoblotting analysis revealed that AhR protein levels were significantly lower in adult livers than in *AhR+/+* preweaning livers; AhR protein remained undetectable at any developmental stage in *AhR−/−* mice (Figure 3F).

Persistent INS-R/PI3K-Dependent Signaling and Sustained ERK1/2 Activation in Non-polyploid AhR-Null Livers

To investigate the possible signaling networks that could mediate the AhR-null liver phenotype, we first focused on the insulin receptor (INS-R) and its downstream PI3K (phosphatidylinositol-3-phosphate kinase) pathway since it is a critical regulator of cell viability, proliferation, and eventually, ploidy (Celton-Morizur et al., 2010; Yu and Cui, 2016). INS-R protein levels did not significantly differ between *AhR+/+* and *AhR−/−* livers in preweaning or adult mice (Figure 4A). Although liver maturation seemed to involve a reduction in INS-R expression, it was AhR independent (Figure 4A). Notably, activation of the major INS-R intermediate protein in the liver phospho-IRS-2 (insulin receptor substrate-2) was significantly higher in *AhR−/−* than in

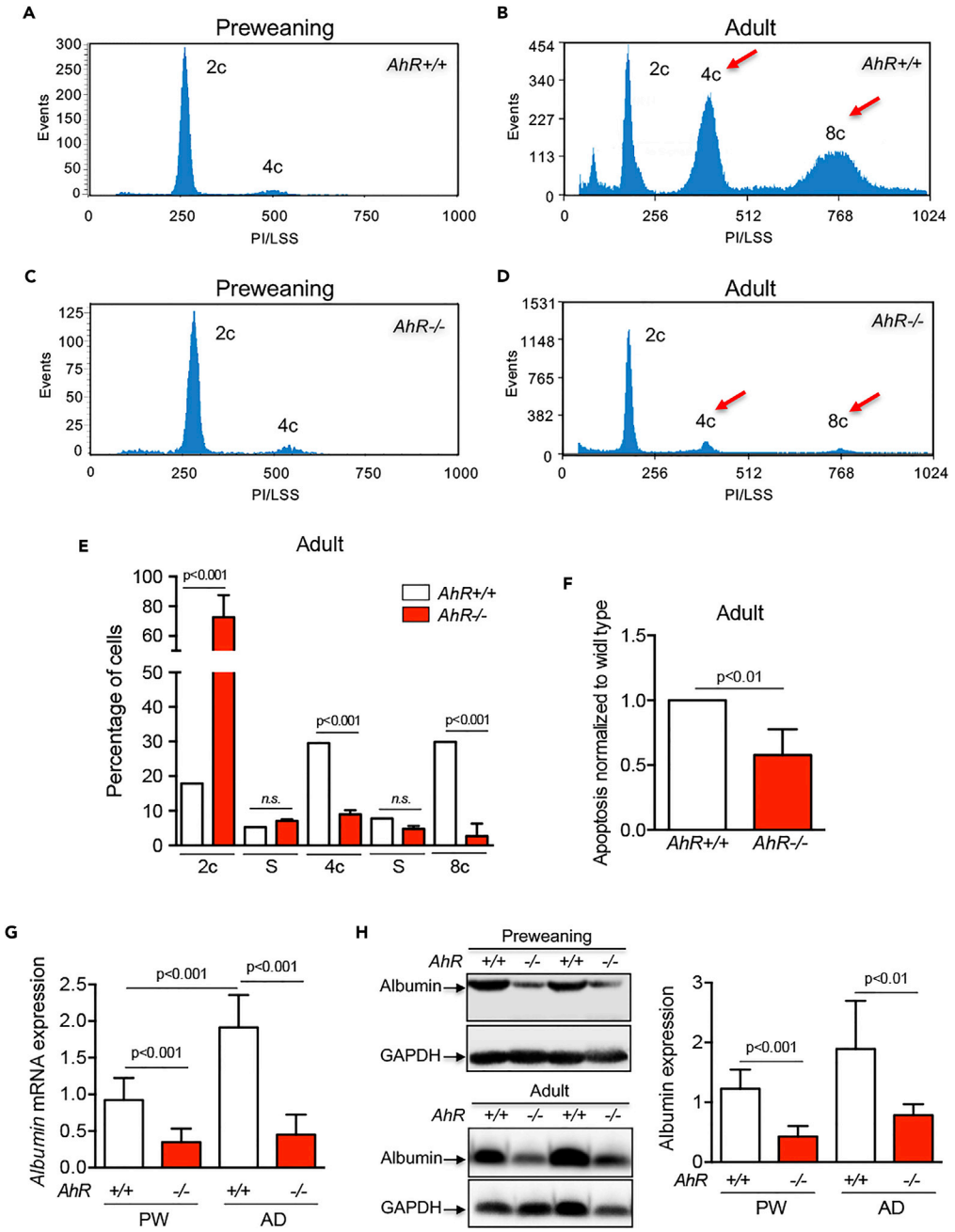

Figure 2. AhR Deficiency Impairs Liver Polyploidy in the Absence of Increased Apoptosis

(A–D) Primary hepatocytes were isolated from preweaning (A and C) and adult (B and D) *AhR+/+* and *AhR−/−* mice by collagenase liver perfusion. Cells were fixed, stained with propidium iodide, and their DNA content analyzed by flow cytometry in a MACSQuant VYB flow cytometer. Peaks correspond to diploid (2c), tetraploid (4c), and octaploid (8c) hepatocytes (red arrows).

(E) Cell subpopulations with different ploidy status were quantified and their percentages represented. Percentage of cells at the S phase (2c-to-4c and 4c-to-8c) transitions are also indicated.

(F) Apoptotic cells in adult *AhR−/−* livers were quantified and normalized by those of *AhR+/+* mice.

(G and H) Albumin mRNA (G) and protein (H) expression was determined in liver tissue from preweaning and adult *AhR+/+* and *AhR−/−* mice. mRNA gene expression was normalized by *Gapdh* and represented as $2^{-\Delta\Delta Ct}$.

Six *AhR+/+* and seven *AhR−/−* mice were analyzed for each developmental time and four technical replicates were performed. Data are shown as mean ± SD. n.s., Not statistically significant; SD, standard deviation. Antibodies and oligonucleotides used are indicated in Tables S1 and S2, respectively. See also Figure S1.

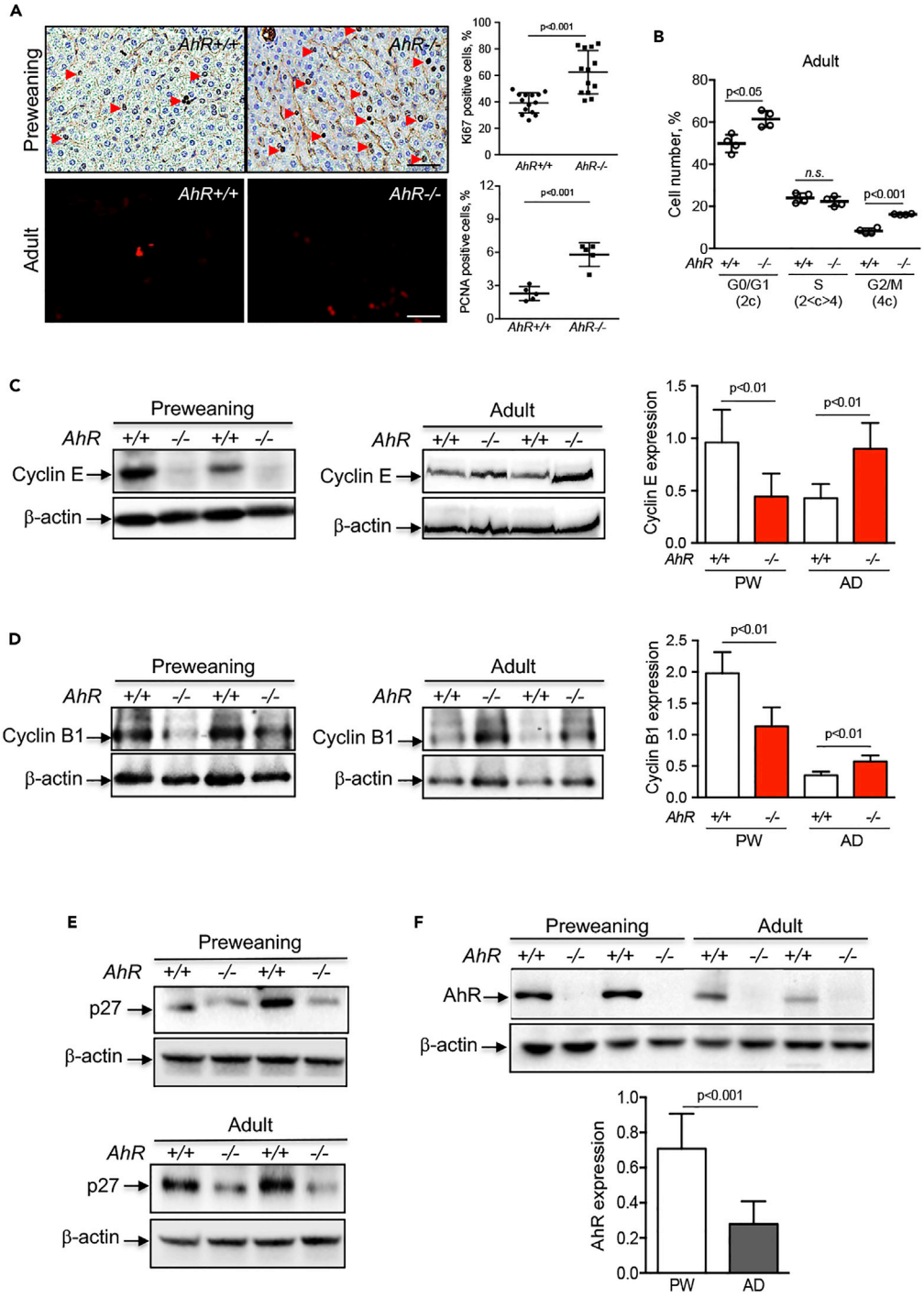

Figure 3. AhR-Null Livers Have Increased Proliferation and Changes in Cell Cycle Regulators Cyclin E and p27^{Kip1}

(A) *In vivo* proliferation was determined in Ki67-stained tissue sections from preweaning *AhR+/+* and *AhR−/−* mouse liver. Adult livers from *AhR+/+* and *AhR−/−* mice were analyzed by confocal multiphoton microscopy using tissue sections stained for the proliferating cell nuclear antigen (PCNA). An Olympus FV1000 confocal microscope (Olympus) equipped with a multiphoton unit was used. Arrowheads mark proliferation positive hepatocytes.

(B) Primary hepatocytes were isolated from adult AhR wild-type and AhR-null mice by collagenase perfusion and freshly analyzed for cell cycle distribution by flow cytometry after staining with propidium iodide. Fraction of cells in G0/G1 (2c), S (2 < c > 4), and G2/M (4c) are represented. A Cytomics FC500 equipment was used.

Figure 3. *Continued*

(C–E) Total protein was obtained from preweaning and adult *AhR+/+* and *AhR−/−* livers and analyzed by immunoblotting for Cyclin B1 (C), Cyclin E (D), and $p27^{Kip1}$ (D) using specific antibodies.

(F) AhR protein expression was also analyzed in preweaning (PW) and adult (AD) liver extracts from *AhR+/+* and *AhR−/−* by immunoblotting. β-Actin was used to confirm protein integrity and equal loading.

Two representative mice for each experimental condition are shown. Seven mice for each developmental time and genotype and three technical replicates were analyzed. Data are shown as mean ± SD. n.s., Not statistically significant; SD, standard deviation. Scale bar, 50 μm. Antibodies used are indicated in Table S1.

AhR+/+ mice at both preweaning and adult age (Figure 4B), suggesting that despite similar receptor levels INS-R signaling might be increased in the absence of AhR. We next decided to address whether INS-R/IRS-2 overactivation was functionally relevant in modulating PI3K signaling in *AhR−/−*liver. The expression levels of the PI3K regulatory subunit, which interacts with phospho-IRS-2, p85α, were significantly increased in preweaning and adult *AhR−/−* livers when compared with *AhR+/+* livers (Figure 4C).

Serine-threonine protein kinase-B/AKT (hereinafter AKT) is the required PI3K signaling intermediate in most cell types (Yu and Cui, 2016). Total protein levels of AKT were not affected by AhR expression at any of the developmental times analyzed. However, active phospho-AKT ($p\text{-}AKT^{Ser473}$) was significantly upregulated by AhR deficiency in both preweaning and adult livers, and total levels in adults exceed those in preweaning mice (Figure 4D). Consistently, p-AKT target protein glycogen synthase kinase-3β (GSK3β) was more efficiently phosphorylated ($p\text{-}GSK3\beta^{Ser9}$) in preweaning and adult *AhR−/−* livers than in their *AhR+/+* counterparts with a pattern closely resembling that of p-AKT (Figure 4E). PI3K activity and AKT phosphorylation are negatively regulated by the phosphatase and tensin homolog (PTEN) (Bunney and Katan, 2010). Accordingly, PTEN was significantly downregulated in preweaning and adult *AhR−/−* livers with a pattern inverse to that found for p-AKT (Figure 4F). Altogether, these results suggest that the increased proliferative potential of *AhR−/−* livers may be associated with a sustained overactivation of the INS-R/PI3K pathway. PI3K also signals to the Ras pathway, ultimately regulating the activation of mitogen-activated protein kinases (MAPKs) involved in cell proliferation, including the extracellular signal-regulated kinases 1/2 (ERK1/2) (Busca et al., 2016; Sturgill, 2008). We observed that the total levels of ERK1 (ERK1/p44) did not significantly change between *AhR+/+* and *AhR−/−* livers in preweaning or adult mice. However, normalized phosphorylated ERK1/p44 levels (pERK/ERK ratio) increased in the absence of AhR under both developmental conditions (Figures 5A and 5B). The ERK2/p42 isoform did not show significant differences in normalized phosphorylation levels between AhR wild-type and AhR-null preweaning mice, although it was upregulated in adult *AhR−/−* livers (Figures 5A and 5C). Thus, sustained PI3K-dependent ERK1/2 signaling may also contribute to altered preweaning-to-adult transition in AhR-deficient liver.

PI3K also signals to inhibit the p53 tumor suppressor to block apoptosis in proliferating cells (Sabbatini and McCormick, 1999; Yamaguchi et al., 2001). Notably, recent studies have also shown that p53 has relevant functions in preventing polyploidy in mature cells (Aylon and Oren, 2011; Kurinna et al., 2013). We then sought to analyze whether liver maturation involved changes in p53 expression in an AhR-dependent manner. Immunoblotting experiments showed that p53 levels were markedly reduced in preweaning *AhR−/−* livers with respect to *AhR+/+* livers (Figure 5D). One of the most relevant targets of active p53 is the $p21^{Cip1}$ protein ($p21^{Cip1}$), also involved in repressing cell proliferation (Jung et al., 2010; Karimian et al., 2016). Accordingly, its expression closely followed that of p53 in preweaning *AhR−/−* and *AhR+/+* livers, being significantly downregulated in AhR-null mice (Figure 5E). Surprisingly, however, p53 expression was higher in adult *AhR−/−* livers than in age-matched *AhR+/+* livers (Figure 5D), despite the persistent $p21^{Cip1}$ repression present in AhR-lacking hepatocytes (Figure 5E). Thus, low p53 levels may allow higher proliferation rates during preweaning in *AhR−/−* mice, whereas its increasing expression in adults could block polyploidy in the absence of a significant inhibitory effect on proliferation.

Lack of Polyploidy in Adult *AhR−/−* Liver Involves Altered Wnt/β-Cat Signaling

The PI3K pathway is also linked to Wnt/β-Cat signaling since the AKT downstream target GSK3β is a component of the Wnt/β-Cat degradation complex (Nusse and Clevers, 2017). Immunofluorescence analysis by confocal microscopy of liver sections from preweaning mice revealed increased levels and a more abundant nuclear localization of β-Cat in the centrilobular areas of the hepatic parenchyma in *AhR−/−* than in *AhR+/+* mice (Figure 6A), in agreement with the zonation of β-Cat in the liver (Benhamouche et al., 2006; Burke et al., 2009). Immunoblotting of nuclear extracts also showed increased levels of β-Cat in AhR-null

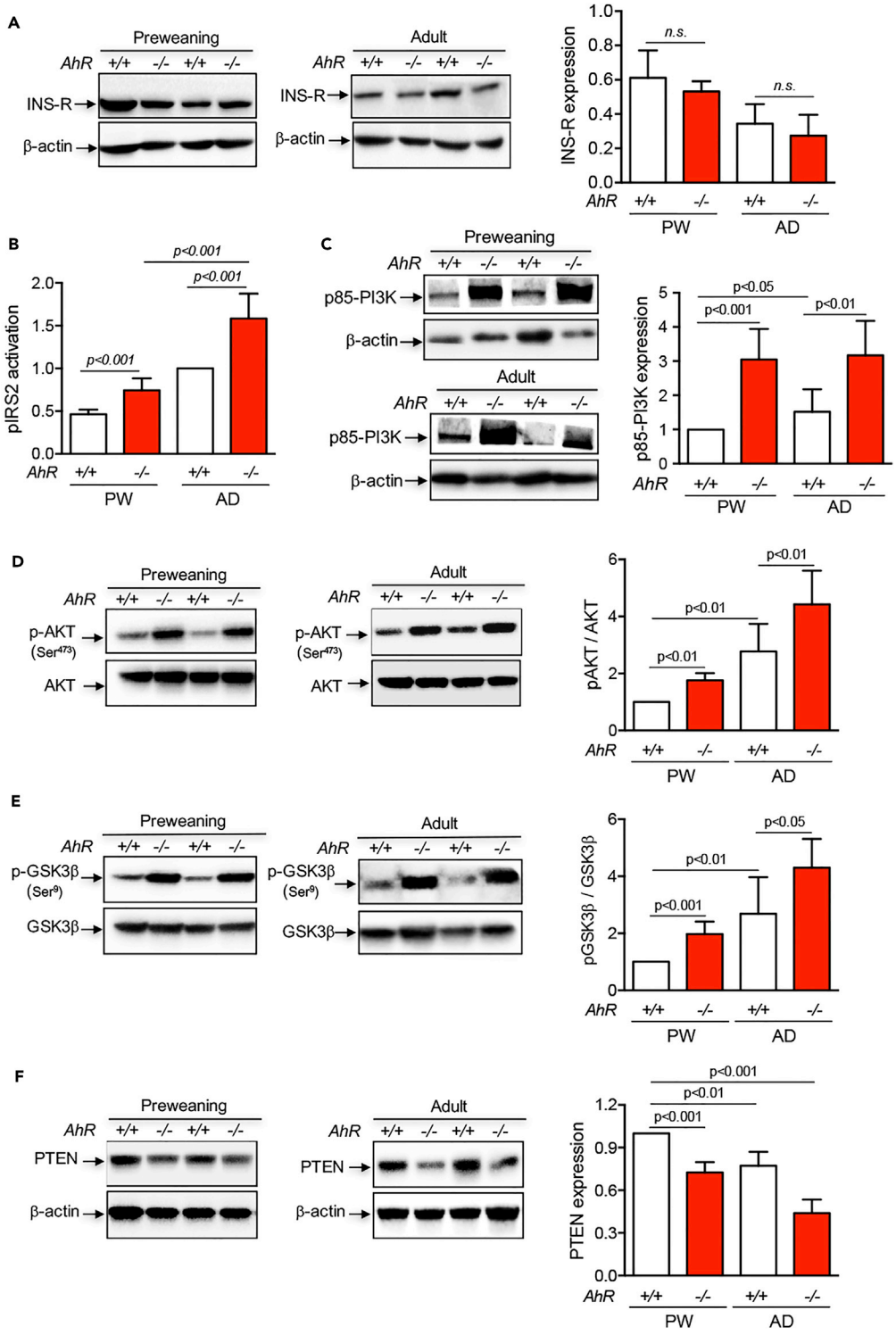

Figure 4. Insulin Receptor Signaling Is Altered in AhR-null Livers and the INS-R/PI3K Pathway May Contribute to the Increased Proliferative Potential of *AhR*−/− Livers

(A) Protein expression of the insulin receptor (INS-R) was analyzed by immunoblotting in liver extracts from preweaning (PW) and adult (AD) *AhR*+/+ and *AhR*−/− mice.

(B) Activation of the INS-R signaling intermediate IRS-2 was quantified by an enzyme-linked immunosorbent assay (ELISA) kit that detects the phosphorylated form of the protein. A positive control was performed using mice treated with insulin.

Figure 4. *Continued*

(C) Protein levels of IRS-2 downstream intermediate p85-PI3K were determined by immunoblotting using the experimental conditions indicated above.

(D and E) Immunoblotting using specific antibodies was used to analyze activation levels of molecular intermediates of the INS-R/PI3K pathway: AKT (total AKT and p-AKT^{Ser473}) (D) and GSK3β (total GSK3β and p-GSK3β^{Ser9}) (E).

(F) Protein levels of the PI3K-negative regulator PTEN were also analyzed by immunoblotting. β-Actin was used to confirm protein integrity and equal loading.

Two representative mice for each experimental condition are shown. Ten mice for each developmental time and genotype and three to four technical replicates were analyzed. Data are shown as mean ± SD. n.s., Not statistically significant; SD, standard deviation. Antibodies used are indicated in Table S1.

preweaning mice (Figure 6A). The difference in β-Cat expression between *AhR+/+* and *AhR−/−* livers was milder in adult mice, and its overall levels were reduced with respect to preweaning mice of either phenotype (Figure 6A). Nevertheless, β-Cat was active in adult *AhR−/−* liver since the mRNA expression of its target genes *Axin*, *Cyclin D1*, *c-Myc,* and *Lef1* was increased with respect to *AhR+/+* adult liver (Figure 6B). Interestingly, co-immunoprecipitation experiments showed that, in fact, AhR may be a component of a protein complex that also includes β-Cat in both preweaning and adult livers (Figure 6C); no significant co-immunoprecipitation between AhR and β-Cat was detected in preweaning or adult *AhR−/−* livers (Figure 6C). In addition, β-Cat seemed to also interact in a common protein complex with activated phospho-AKT in preweaning and adult livers and with increased efficiency in *AhR−/−* mice (Figure 6D). Thus, *in vivo*, upregulated AKT and β-Cat signaling may cooperate to maintain hepatocyte proliferation and to reduce their ploidy in the absence of AhR expression.

To further investigate if AhR modulates Wnt/β-Cat signaling in adult liver, primary hepatocytes were isolated from *AhR+/+* and *AhR−/−* mice by collagenase perfusion and cultured in cell medium containing hepatocyte growth factor (HGF) and epidermal growth factor (EGF). Experiments were done in the presence of conditioned medium enriched in the Wnt/β-Cat ligand Wnt3a or after treatment with the AhR non-toxic agonist 6-formylindolo[3,2-b]carbazole (FICZ). mRNA expression of the β-Cat target gene *Axin2* was moderately induced by Wnt3a but not by FICZ in AhR wild-type hepatocytes; by contrast, Wnt3a treatment markedly increased *Axin2* mRNA in AhR-null primary hepatocytes (Figure 6E). AhR target gene *Cyp1a1* was largely induced by FICZ and significantly by Wnt3a in *AhR+/+* primary hepatocytes; no significant *Cyp1a1* expression was detected in *AhR−/−* primary hepatocytes (Figure 6E). Thus, the transcriptional activity of AhR can be induced by Wnt/β-Cat signaling in AhR-expressing primary hepatocytes, but not vice versa, and interestingly, AhR-lacking primary hepatocytes were highly responsive to activation of the Wnt/β-Cat pathway. To give additional support to these data, primary hepatocytes from *AhR+/+* and *AhR−/−* livers were transfected with a TOP-Flash reporter construct that allows quantification of β-Cat-dependent transcription. TOP-Flash luciferase activity was higher in adult *AhR−/−* primary hepatocytes under basal culture conditions (Figure 6F), and more notably after treatment with Wnt3a-enriched medium (Figure 6F). Transfection of the TOP-Flash reporter construct in preweaning primary hepatocytes also revealed an increase in β-Cat transcriptional activity in *AhR−/−* cells (Figure 6G).

Conserved mTOR Activation during the Preweaning-to-Adult Transition in the Liver

Different signaling pathways controlling cell proliferation, metabolism, and differentiation converge to the mammalian target of rapamycin (mTOR). Particularly relevant are those mediated by PI3K, ERK, and Wnt/β-Cat, which activate the mTORC1 complex through the guanosine triphosphate (GTP)-binding protein RHEB (Laplante and Sabatini, 2009, 2012; Saxton and Sabatini, 2017). We therefore decided to determine whether the sustained activation of those pathways in the preweaning-to-adult transition in *AhR−/−* liver resulted in increased mTORC1 activation. Protein analysis showed that mTOR expression remained at a higher level in both preweaning and adult *AhR−/−* livers when compared with their counterpart *AhR+/+* livers (Figure 7A). One major target of the mTORC1 complex is the ribosomal S6 kinase-1 (S6K1), which is activated by phosphorylation (Laplante and Sabatini, 2009, 2012; Saxton and Sabatini, 2017). In addition to its functions in protein synthesis, S6K1 has been recently implicated in the control of polyploidy (Ma et al., 2009). The levels of phosphorylated S6K1 were increased in preweaning and adult *AhR−/−* livers when compared with *AhR+/+* liver (Figure 7B), in agreement with the observed pattern of mTOR expression. Hence, the persistent activation of INS-R/PI3K/ERK and Wnt/β-Cat signaling pathways that takes place during liver maturation in *AhR−/−* mice might assemble at the mTORC1 complex, maintaining proliferation and inhibiting differentiation-related polyploidy.

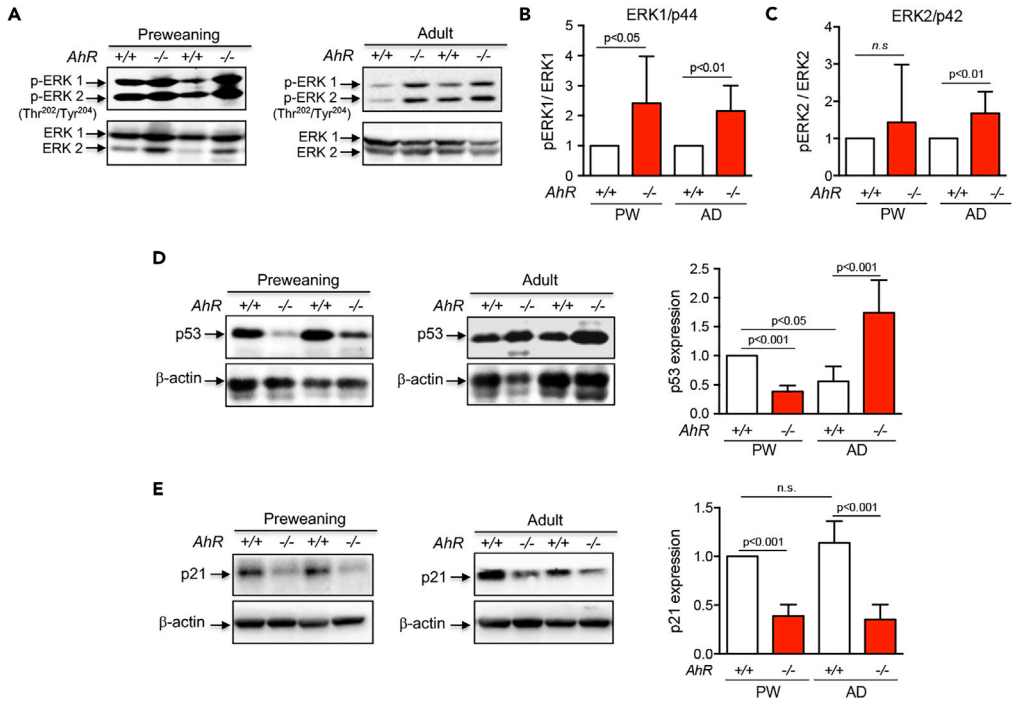

Figure 5. Liver Maturation Involves Changes in ERK1/2, p53, and p21^{Cip1}

(A–E) Preweaning (PW) and adult (AD) *AhR+/+* and *AhR−/−* livers were processed to obtain total protein extracts that were analyzed by immunoblotting for total and phosphorylated ERK1/p44 and ERK2/p42 (ERK1/2, p-ERK1/2$^{Thr202/Tyr204}$) (A–C), p53 (D), and p21^{Cip1} (E). β-Actin was used to confirm protein integrity and equal loading. Two representative mice for each experimental condition are shown. Ten mice for each developmental time and genotype and three technical replicates were analyzed. Data are shown as mean ± SD. n.s., Not statistically significant; SD, standard deviation. Antibodies used are indicated in Table S1.

AhR Deficiency Alters Metabolic Parameters Associated with Polyploidy and mTOR Activity

The PI3K-mTOR pathway has relevant functions in metabolism and energy control (Saxton and Sabatini, 2017; Yu and Cui, 2016). Recent work suggests that mTOR inhibition reduces glycolytic metabolism in polyploid cells (Liu et al., 2013) and that amino acids such as L-Leu may regulate mTORC1 activity in certain forms of anemia (Boultwood et al., 2013; Payne et al., 2012). We then performed metabolome analysis for amino acid content in serum from preweaning and adult *AhR+/+* and *AhR−/−* mice. Interestingly, L-Leu was significantly enriched in *AhR−/−* preweaning serum when compared with *AhR+/+* mice, although no significant changes were observed in adult mice (Figure 7C). L-Gln, which cooperates in transporting L-Leu into the cell, had also significantly higher levels in preweaning *AhR−/−* mice serum and a tendency of accumulation in adult AhR-null mice (Figure 7D). It is thus possible that L-Leu/L-Gln may contribute to mTORC1 activation in preweaning liver. We next did metabolomics for intermediates of the mitochondrial oxidative phosphorylation to determine whether reduced polyploidy in *AhR−/−* liver favors oxidative versus glycolytic metabolism. The results showed significant increases in serum levels of aerobic metabolism intermediates succinate, fumarate, and malate during the preweaning-to-adult transition in *AhR−/−* mice when compared with *AhR+/+* mice (Figure 7E), in agreement with the prominent roles of succinate (and to a lesser extent fumarate) in providing cellular energy and blocking senescence in replicative cells (Chen et al., 2015), and with the preferred glycolytic metabolism found in high-ploidy cells (Liu et al., 2013). Moreover, azelaic acid monoesters, which are negatively regulated by the hepatic carboxylesterase-3 (CES3) in an AhR-dependent manner and which could contribute to the liver steatosis present in very young *AhR−/−* mice (Matsubara et al., 2012), were also markedly upregulated in preweaning *AhR−/−* liver, concomitantly to an inhibition of CES3 expression (Figures 7F and 7G).

Lack of Polyploidy in Adult AhR-Null Liver May Be Related to Centrosome Amplification

In the liver, developmental polyploidy may arise after several rounds of genome duplication in the absence of cytokinesis (Pandit et al., 2013), with the appearance of supernumerary centrosomes (Conduit et al.,

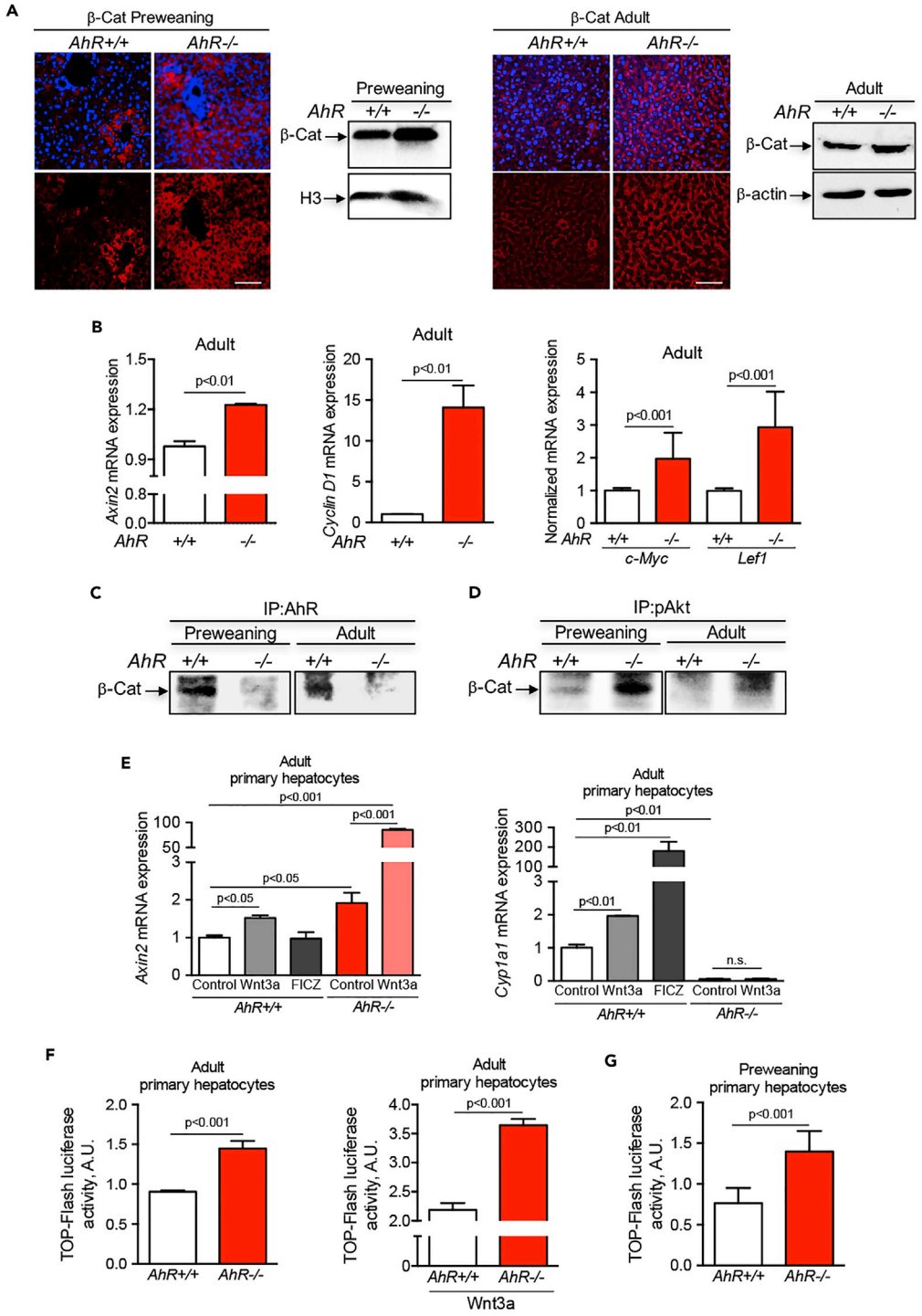

Figure 6. β-Cat Expression and Signaling Are Upregulated in AhR-Deficient Liver and AhR Modulates Wnt/β-Cat-Dependent Transcription in Mouse Primary Hepatocytes

(A) Liver tissue was obtained from preweaning and adult *AhR+/+* and *AhR−/−* mice, fixed, embedded in paraffin, sectioned, and analyzed by immunofluorescence for β-Cat expression using a specific primary antibody and an Alexa 633-labeled secondary antibody. Sections were visualized using an Olympus FV1000 confocal microscope (Olympus). DAPI was used to label cell nuclei. Nuclear extracts (A, left panel) and total liver protein (A, right panel) were also analyzed for β-Cat protein levels by immunoblotting using a specific antibody.

Figure 6. *Continued*

(B) Total RNA was purified from adult *AhR+/+* and *AhR−/−* liver, reverse transcribed, and mRNA gene expression for the β-Cat target genes *Axin2*, *Cyclin D1*, and *c-Myc* and *Lef1* were quantified by real-time quantitative polymerase chain reaction (qPCR) using the oligonucleotides indicated in Table S1.

(C and D) Total liver protein from preweaning (PW) and adult (AD) *AhR+/+* and *AhR−/−* mice was immunoprecipitated for AhR (C) or pAKT (D) and the presence of β-Cat in the complexes detected by immunoblotting using a specific antibody. Adult primary hepatocytes were isolated from *AhR+/+* and *AhR−/−* mice by collagenase perfusion and cultured in complete medium containing HGF and EGF.

(E) Adult *AhR+/+* primary hepatocytes were treated with medium from control L1 cells (control), medium from L1-Wnt3a-producing cells (1:4 dilution), or 10 μM FICZ. *AhR−/−* primary hepatocytes were treated with medium from control L1 cells (control) or medium from L1-Wnt3a-producing cells (1:4 dilution). Total RNA was purified and analyzed for *Axin2* or *Cyp1a1* mRNA expression by reverse-transcriptase (RT)-qPCR.

(F) Adult primary hepatocytes from *AhR+/+* and *AhR−/−* liver were transfected with the TOP/FOP luciferase system to determine β-Cat-dependent transcription under basal cell conditions or after treatment with L1-Wnt3a conditioned medium (1:4 dilution).

(G) The TOP/FOP luciferase assay was also performed in preweaning primary hepatocytes obtained from mice of either genotype. mRNA gene expression was normalized by *Gapdh* and represented as $2^{-\Delta\Delta Ct}$. β-Actin and histone H3 (H3) were used to confirm protein integrity and equal loading. Eight mice for each developmental time and genotype and at least three technical replicates were analyzed.

Data are shown as mean ± SD. n.s., Not statistically significant; SD, standard deviation. Scale bar, 50 μm. Antibodies and oligonucleotides used are indicated in Tables S1 and S2, respectively.

2015). Interestingly, continued expression of endogenous AhR was shown to promote centrosome amplification (e.g., increased number of centrosomes) in breast cancer cells (Korzeniewski et al., 2010). We considered the possibility that low-ploidy *AhR−/−* livers may have altered centrosome organization. Pericentrin (PCN), a prototypical component of the pericentriolar material (PCM) surrounding the centriole, was overexpressed in preweaning and adult *AhR−/−* livers with respect to *AhR+/+* liver, as determined by immunoblotting (Figure 8A). Confocal immunofluorescence in liver sections stained for PCN showed that, in the absence of AhR, adult hepatocytes appeared to have larger and strongly stained centrosomes than *AhR+/+* adult livers (Figure 8B). Image analyses were performed to quantify the area and volume of the centrosomes in *AhR+/+* and *AhR−/−* livers. In agreement, centrosomes of *AhR−/−* livers had larger areas (Figure 8C) and volumes (Figure 8D) than centrosomes in *AhR+/+* livers.

Pharmacological Inhibition of PI3K, ERK, and Wnt/β-Cat Signaling Partially Rescues Polyploidy in *AhR−/−* Liver

We next decided to investigate if inhibition of PI3K, ERK, and Wnt/β-Cat signaling could rescue polyploidy in *AhR−/−* liver (Figure 9). Primary hepatocytes were isolated from *AhR+/+* and *AhR−/−* mice by collagenase perfusion and cultured in the presence of pharmacological inhibitors LY294002 (PI3K), PD98059 (ERK), and salinomycin (Wnt/β-Cat). Inhibition of these signaling pathways increased the number of hepatocytes with 4c DNA content in both genotypes and interestingly, stimulated the appearance of *AhR−/−* hepatocytes with >4c DNA content, including octaploid cells (Figures 9A and 9B).

Treatment of *AhR−/−* mice with these inhibitors *in vivo* for 7 days reduced signaling through PI3K as determined by AKT phosphorylation at Ser473 (Figure 9C) and downregulated the expression of mTOR with respect to untreated AhR-null mice (Figure 9D). Overall, these *in vitro* and *in vivo* experiments support the involvement of PI3K, ERK, and Wnt/β-Cat signaling in liver polyploidization through a mechanism requiring AhR expression.

DISCUSSION

Taking into account that AhR expression promotes differentiation in different cell types (Esser and Rannug, 2015; Mulero-Navarro and Fernandez-Salguero, 2016), and since polyploidization is in fact a differentiation process, we decided to investigate the role of AhR in the transition from a preweaning diploid liver to an adult polyploid liver and the signaling pathways that might be involved. The main conclusion from this work is that AhR maintains the activation of signaling pathways controlling proliferation, differentiation, and metabolism within physiological levels for proper liver polyploidization and maturation. The fact that several related pathways are modulated by AhR to control physiological liver polyploidy suggests that this receptor may be acting as a downstream hub in the signaling network. Future studies are guaranteed

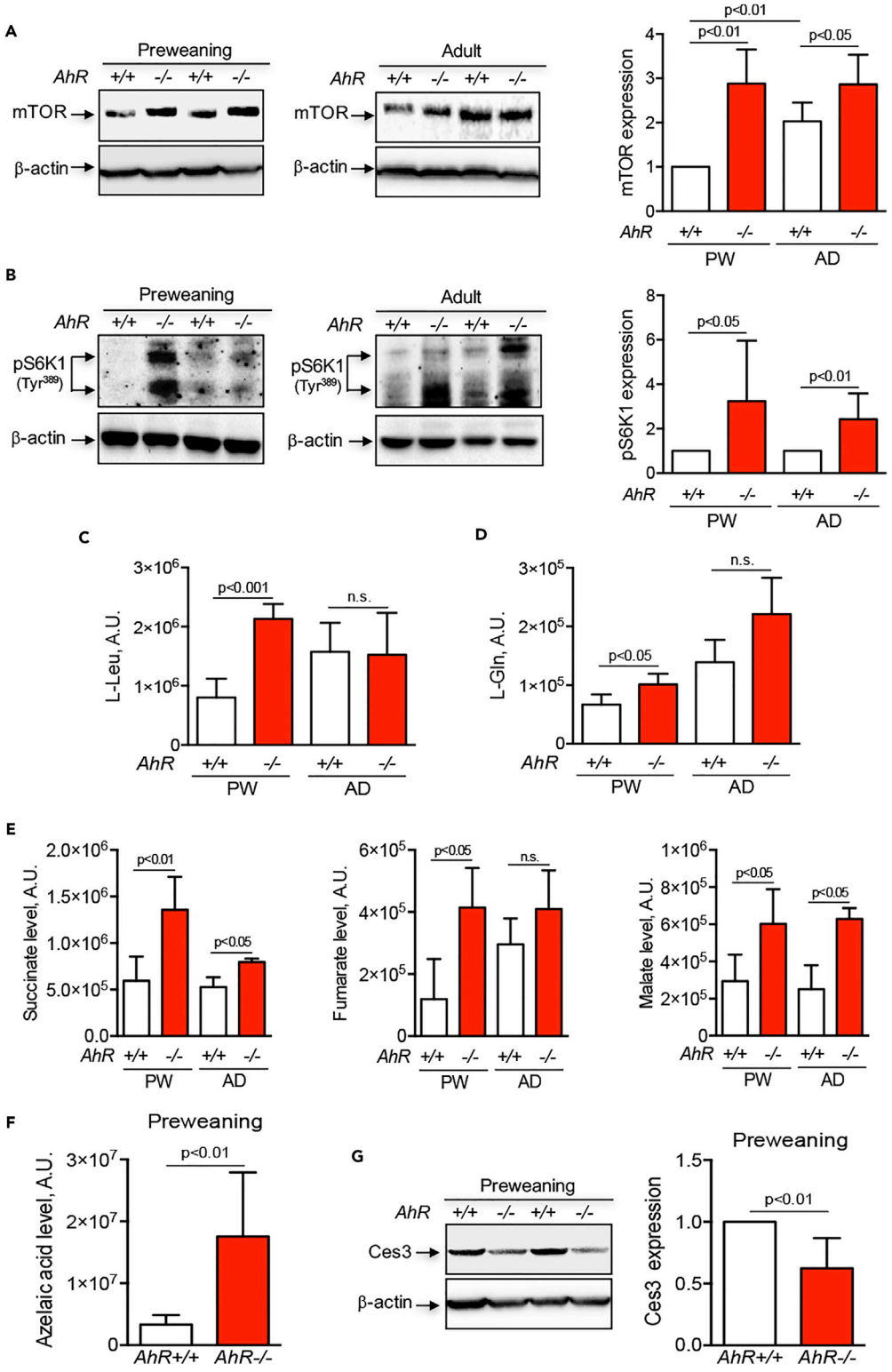

Figure 7. mTOR Expression, Ribosomal S6K1 Activation, and Metabolomic Changes during the Preweaning-to-Adult Transition in *AhR*−/− Liver

(A) Total protein obtained from preweaning (PW) and adult (AD) *AhR*+/+ and *AhR*−/− liver were analyzed for the expression of mTOR by immunoblotting using a specific antibody.

Figure 7. *Continued*

(B–D) (B) Protein extracts from the same mice were used to determine by immunoblotting the level of activation of mTORC1 target protein phospho-S6K1 (p-S6K1^{Tyr389}). Serum samples were obtained from preweaning (PW) and adult (AD) *AhR+/+* and *AhR−/−* mice, processed, and their metabolites analyzed by chromatographic separation and mass spectrometry. The levels of mTORC1-activating amino acids L-Leu (C) and L-Gln (D) were measured and quantified in both AhR genotypes and developmental stages.

(E) Metabolomics were also used to identify and quantify the accumulation of intermediates of the mitochondrial oxidative metabolism succinate, fumarate, and malate in the samples indicated above.

(F) Levels of azelaic acid were determined by chromatography and mass spectrometry in serum samples from preweaning *AhR+/+* and *AhR−/−* mice.

(G) Protein levels of the hepatic carboxylesterase-3 (CES3) were determined in preweaning *AhR+/+* and *AhR−/−* mice by immunoblotting using a specific antibody. β-Actin was used to confirm protein integrity and equal loading.

Two representative mice for each experimental condition are shown. Eight mice (A–D) or six mice (E–F) for each developmental time and genotype and three technical replicates were analyzed. Data are shown as mean ± SD. Antibodies used are indicated in Table S1. SD, standard deviation.

to determine the relative contribution of each of these pathways to the phenotype and the precise points for AhR interaction.

AhR deficiency increased the cellularity and reduced the average cell size in the preweaning proliferating liver and surprisingly, such hyperproliferative phenotype, rather than being blocked as in AhR wild-type mice, persisted in adult *AhR−/−* livers as demonstrated by Ki67 and PCNA immunodetection. These observations suggest that AhR is needed to maintain cell growth and proliferation within adequate physiological ranges in early stages of postnatal liver development. Even more, since the preweaning-to-adult transition involves a process of differentiation by which hepatocytes modify their cell cycle to inhibit division (Celton-Morizur et al., 2010; Sigal et al., 1999; Zielke et al., 2013), it appears likely that AhR is also required to switch from a proliferative to a differentiated adult liver. This hypothesis is supported by the fact that the liver differentiation marker albumin reached much higher expression levels in polyploid *AhR+/+* livers than in mostly diploid *AhR−/−* livers. In addition, it is also known that AhR is able to prevent mitotic progression, induce differentiation, and inhibit pluripotency in different cell types (Contador-Troca et al., 2013; Esser and Rannug, 2015; Ko et al., 2016; Morales-Hernandez et al., 2016; Mulero-Navarro and Fernandez-Salguero, 2016).

Increased cell size, reduced proliferation, and terminal differentiation are common properties of polyploid cells including hepatocytes (Conlon and Raff, 1999; Raff, 1996). We therefore questioned whether AhR could be relevant for polyploidization of the adult liver. Indeed, AhR depletion maintained a predominantly diploid adult liver with a high content of mononuclear hepatocytes, suggestive of impaired polyploidy. To date, a sole single report has suggested that AhR may be needed for the differentiation and polyploidization of mouse megakaryocytes (Lindsey and Papoutsakis, 2011). The existence of this common function of AhR in different unrelated cell types emphasizes that ploidy maintenance may be an evolutionary conserved role for this receptor along phylogeny. The implication of AhR in inducing differentiation and polyploidy was further supported by the fact that, in the absence of AhR, compromised polyploidy in adult mice was accompanied by upregulation of cell cycle proteins promoting transition through G1/S and G2/M, Cyclin B1 and Cyclin E, and repression of cell cycle inhibitors p27^{Kip1} and p21^{Cip1}. Thus, adult mice liver polyploidy could involve physiological control of the cell cycle by a process requiring AhR expression. Consistently, since AhR can bind to inactive hypophosphorylated retinoblastoma protein (pRB) and to displace p300 from E2F promoters, AhR deficiency may result in enhanced proliferation in adult hepatocytes. Interestingly, lack of E2F8 transcription factor impairs polyploidization in mouse liver through overexpression of E2F-dependent target genes (Pandit et al., 2012), thus producing a phenotype similar to that present in AhR-null mice. Since the E2F8-deficient phenotype was associated with the upregulation of pro-cytokinesis genes, it might be relevant to address to what extent cytokinesis affects ploidy in *AhR−/−* mouse liver. It is intriguing that preweaning *AhR+/+* mice maintained higher levels of Cyclin B1 and Cyclin E despite their reduced proliferative potential with respect to *AhR−/−* mice. One possible explanation for these results is that wild-type livers overexpress positive regulators of the cell cycle to overcome their increased content in negative regulators p27^{Kip1} and p21^{Cip1}.

Although the reduced polyploidy present in adult AhR-null liver could result from defective endoreplication (Zielke et al., 2013), it is also possible that the so-called ploidy reversal (Duncan et al., 2010) could generate cells of variable ploidy from a fraction of mature *AhR−/−* polyploid hepatocytes, ultimately

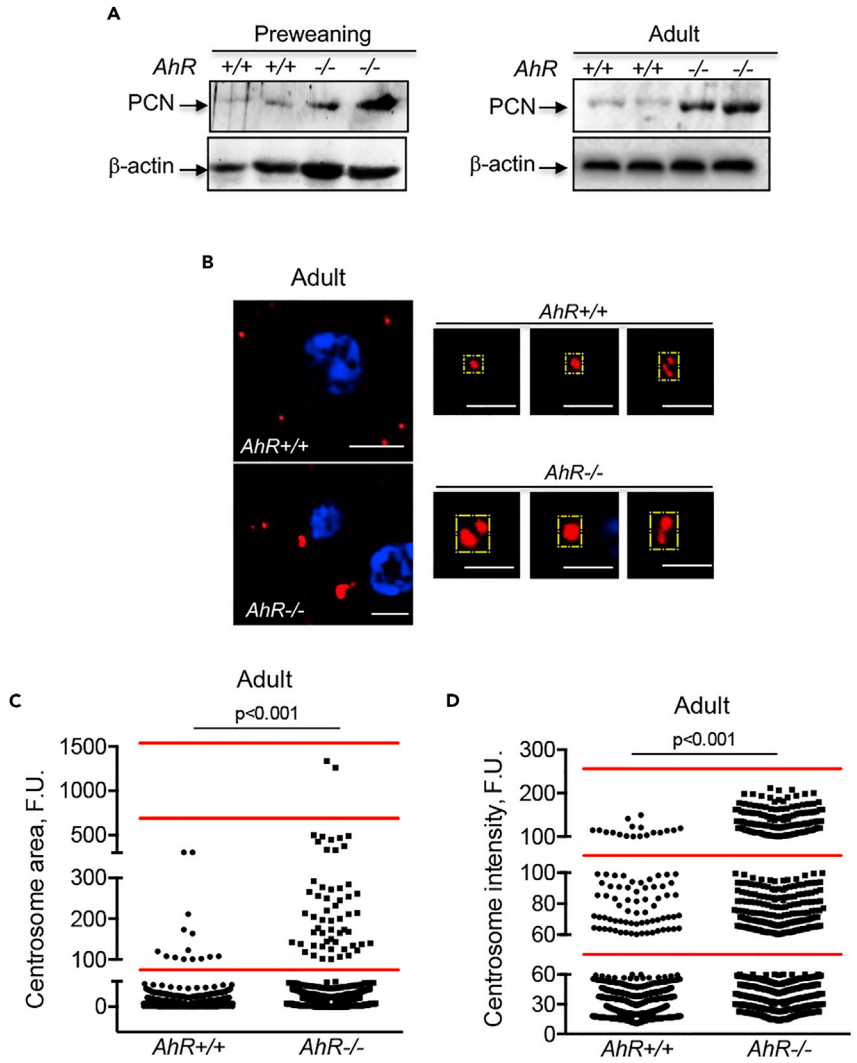

Figure 8. Lower Ploidy in *AhR*−/− Liver Could Be Associated with Altered Centrosome Composition

(A) Total protein was obtained from preweaning and adult *AhR*+/+ and *AhR*−/− liver and analyzed for pericentrin (PCN) expression by immunoblotting using a specific antibody.

(B) Livers from adult *AhR*+/+ and *AhR*−/− mice were fixed, embedded in paraffin, sectioned, and analyzed for PCN expression by immunofluorescence using a specific primary antibody and an Alexa 633-labeled secondary antibody. Sections were visualized using an Olympus FV1000 confocal microscope (Olympus). DAPI was used to label cell nuclei. Details of centrosomes at higher magnification are shown within yellow boxes on the right panels.

(C and D) Centrosomal area (C) and PCN protein amount (D) were quantified using the ImageJ software, and the data show the different ranges in which centrosomes can be clustered for each mice genotype. β-Actin was used to confirm protein integrity and equal loading.

Two representative mice for each condition are shown. Six mice for each developmental time and genotype and four technical replicates were analyzed. Data are shown as mean ± SD. Scale bar, 15 μm. Antibodies used are indicated in Table S1. SD, standard deviation.

restoring proliferative potential. Among the several molecular mechanisms driving polyploidy, failure to complete cytokinesis after mitosis appears relevant in mammalian liver (Zielke et al., 2013). We have found that the levels of PCN, a component of the PCM with relevant roles in spindle organization (Zimmerman et al., 2004), was restricted in centrosomes of AhR-expressing hepatocytes, suggesting that control of centrosomal activity by AhR may contribute to reduced proliferation and increased polyploidy. Since increased centrosome size appears related to a higher proliferative potential, adult diploid *AhR*−/− hepatocytes could enlarge their centrosomes to maintain proliferation in the absence of polyploidy. In addition, as

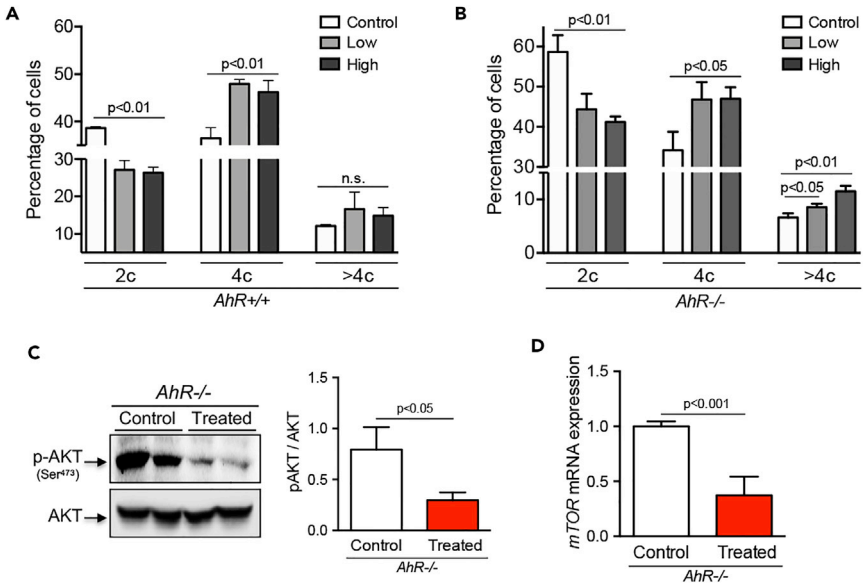

Figure 9. Pharmacological Inhibition of PI3K, ERK, and Wnt/β-Cat Signaling Partially Rescues Polyploidy in *AhR−/−* Liver

(A and B) Primary hepatocytes from *AhR+/+* (A) and *AhR−/−* (B) mice were cultured for 48 hr in the presence of inhibitors for PI3K (LY294002), ERK (PD98059), and Wnt/β-Cat (salinomycin) at a low or high concentration (see Methods). Their DNA content was analyzed by flow cytometry and represented as 2c, 4c, and >4c containing cells.

(C) *AhR−/−* mice were treated *in vivo* with those inhibitors (see Methods), and the activation of PI3K signaling determined by the levels of p-AKT^{Ser473} with respect to total AKT expression.

(D) mTOR expression was also determined *in vivo* under the same experimental conditions indicated above.

Two representative mice for each condition are shown. Six mice of each genotype were perfused to isolate primary hepatocytes for *in vitro* experiments and five mice were treated with inhibitors *in vivo*. Three technical replicates were analyzed. Data are shown as mean ± SD. Scale bar, 15 μm. Antibodies and oligonucleotides used are indicated in Tables S1 and S2, respectively. SD, standard deviation.

PCN regulates mitotic responses in DNA damaged cells (Antonczak et al., 2016), AhR-null hepatocytes could widen their centrosomes to complete cell division under enforced non-polyploid conditions, whereas polyploid AhR wild-type hepatocytes would keep an increased number of smaller centrosomes. Interestingly, lack of the E2F8 transcription factor in mouse liver promotes overexpression of E2F-dependent target genes and enhanced cytokinesis with impaired polyploidization (Pandit et al., 2012). Since such phenotype was related to the upregulation of pro-cytokinesis genes, it could be relevant to address whether pro-cytokinesis genes are also deregulated in *AhR−/−* mouse liver. In addition, altered E2F transcriptional activity could also be involved in the mechanism since AhR inhibits cell proliferation by repressing E2F-dependent transcription through p300 displacement.

Insulin hormone signals through the INS-R to PI3K and Ras-ERK pathways to control cell survival, proliferation, and metabolism (Yu and Cui, 2016). A previous study has shown that AKT activation induced polyploidy in Wistar rat liver (Celton-Morizur et al., 2009, 2010). Our characterization of the INS-R/PI3K/AKT/GSK3β and ERK axes indicated that it was persistently downregulated from preweaning-to-adult *AhR+/+* liver when compared with AhR-deficient liver, suggesting that reduced signaling through those pathways may compromise proliferation and promote polyploid differentiation. In addition, diminished INS-R/PI3K/AKT/GSK3β and ERK signaling in polyploid AhR wild-type liver can be partly explained by the reduced insulin sensitivity of *AhR+/+* with respect to *AhR−/−* mice (Wang et al., 2011). Remarkably, tumor suppressor p53, which is negatively regulated by PI3K signaling (Sabbatini and McCormick, 1999; Yamaguchi et al., 2001), was downregulated in preweaning *AhR−/−* liver but overexpressed in adults. Nonetheless, p53 target gene p21^{Cip1} was consistently suppressed in AhR-null livers at either developmental stage. These apparently contradictory results can be explained in the context of p53-regulating ploidy (Aylon and Oren, 2011; Kurinna et al., 2013) or in the proposed p53-dependent versus p53-independent regulation of p21^{Cip1} (Karimian et al., 2016; Macleod et al., 1995). Since previous work has indicated

that p53 overexpression blocks polyploidy (Aylon and Oren, 2011; Kurinna et al., 2013), it can be suggested that high p53 expression impairs the diploid-to-polyploid transition in adult AhR-null liver, whereas a reduction in p53 levels could positively influence polyploidy in adult *AhR+/+* liver. In addition, $p21^{Cip1}$ could be downregulated independently on p53 in AhR-null liver, as previously reported in *p53−/−* mouse (Macleod et al., 1995).

AhR cross talks with Wnt/β-Cat signaling as AhR activation represses Wnt/β-Cat-related tissue regeneration in zebrafish (Mathew et al., 2009), differentiation of liver progenitor cells (Prochazkova et al., 2011), and early differentiation of mouse embryonic stem cells (Wang et al., 2016). On the other hand, Wnt/β-Cat signaling can increase the expression of AhR target genes in primary human hepatocytes (Gerbal-Chaloin et al., 2014). Wnt/β-Cat signaling was significantly reduced in adult primary *AhR+/+* hepatocytes, suggesting in agreement with earlier data that inhibition of this pathway may contribute to polyploidization. An intriguing possibility is that AhR may be a component of the β-Cat repressive complex since both proteins co-immunoprecipitate under basal conditions in adult *AhR+/+* liver. It is thus plausible that the presence of AhR in the β-Cat complex negatively affects Wnt/β-Cat-dependent functions, including inhibition of cell proliferation. Since active p-AKT co-immunoprecipitated with β-Cat and such effect was more noticeable and sustained in *AhR−/−* than in *AhR+/+* liver, it is possible that cooperation between PI3K and Wnt/β-Cat supports liver proliferation and impairs polyploidy in the absence of AhR. Indeed, INS-R/PI3K can induce Wnt/β-Cat responses by inhibiting GSK3β (Yu and Cui, 2016), which was repressed in adult *AhR−/−* liver.

PI3K/AKT, ERK, and Wnt/β-Cat pathways converge to regulate mTORC1, which is a major complex in controlling proliferation, survival, and metabolism (Laplante and Sabatini, 2009, 2012; Yu and Cui, 2016). Consistently, reduced activation of these pathways in preweaning and adult *AhR+/+* livers coincided with lower mTOR expression and diminished activation of its canonical target S6K1. Altogether, we propose that AhR-expressing hepatocytes inhibit signaling from PI3K/AKT, ERK, and Wnt/β-Cat to mTORC1 to block proliferation, induce differentiation, and trigger polyploidy during the preweaning-to-adult transition. In fact, expression of a kinase-dead form of S6K1 in megakaryocytes increases polyploidy, whereas its rapamycin-resistant active form decreased polyploidy (Ma et al., 2009). mTORC1 also has relevant roles in cellular metabolism, and its activity can be increased by intracellular amino acids (Carroll et al., 2017). AhR expression reduced L-Leu and L-Gln levels in preweaning and L-Gln levels in adult liver. Since L-Leu and L-Gln are co-transported into the cell to activate mTORC1 (Boultwood et al., 2013; Laplante and Sabatini, 2009; Payne et al., 2012), it is possible that reduced L-Leu and L-Gln levels adversely affect mTORC1 in *AhR+/+* polyploid liver. Furthermore, high L-Gln levels in adult *AhR−/−* liver may depend on Wnt/β-Cat since this pathway regulates L-Gln metabolism in the liver (Cadoret et al., 2002).

Polyploidization has been shown to favor glycolytic metabolism over mitochondrial oxidative phosphorylation in acute myeloid leukemia (Liu et al., 2013). Polyploid, low-proliferating *AhR+/+* liver had reduced levels of succinate, considered the most energetic molecule of the mitochondrial aerobic metabolism (Chen et al., 2015). This result suggests that polyploid adult AhR wild-type liver may have a preferred glycolytic energy demand and a more differentiated status than the diploid proliferative adult AhR-null liver that would favor a more energetic mitochondrial metabolism. Finally, preweaning *AhR+/+* livers had reduced levels of azelaic acid, likely due to overexpression of the AhR-regulated CES3 gene. Since high levels of azelaic acid have been associated with steatohepatitis (Matsubara et al., 2012), these data could help explain the steatosis described in postnatal *AhR−/−* mice (Schmidt et al., 1996).

We propose that AhR is needed to establish a physiological control of signaling pathways regulating cell proliferation, differentiation, metabolism, and polyploidy in mouse liver. This hypothesis is supported by the fact that inhibition of PI3K, ERK, and Wnt/β-Cat signaling rescues, at least partially, polyploidy in *AhR−/−* hepatocytes. Since polyploidization is a recurrent trait of human cancer (Zack et al., 2013), understanding how AhR expression influences ploidy may provide novel therapeutic opportunities using non-toxic AhR modulators. Because the pathways identified here are regulated within the same developmental window, it seems reasonable that AhR acts downstream of mTOR, PKB, ERK, and β-Cat possibly by acting as a common intermediate. This may lead to identify novel nuclear and non-nuclear functions of AhR, as previously found for the regulation of caveolin-1, β1-integrin, and c-Src (Enan and Matsumura, 1996; Rey-Barroso et al., 2013, 2014). Elucidating whether ploidy reversal contributes to the reduced polyploidy of adult *AhR−/−* liver represents another relevant question that deserves further investigation.

METHODS

All methods can be found in the accompanying Transparent Methods supplemental file.

SUPPLEMENTAL INFORMATION

Supplemental Information includes Transparent Methods, one figure, and two tables and can be found with this article online at https://doi.org/10.1016/j.isci.2018.05.006.

ACKNOWLEDGMENTS

This work was supported by grants to P.M.F.-S. from the Spanish Ministry of Economy and Competitiveness (SAF2014-51813-R and SAF2017-82597-R) and from the Junta de Extremadura (GR15008 and IB160210). Research at the laboratory of P.M.F.-S. was also funded by the Red Temática de Investigación Cooperativa en Cáncer (RTICC), Carlos III Institute, and Spanish Ministry of Economy and Competitiveness (RD12/0036/0032). N.M.-M. was supported by the Ministerio de Economía y Competitividad. All Spanish funding is co-sponsored by the European Union FEDER Program. The authors acknowledge the support of the Servicio de Técnicas Aplicadas a las Biociencias (STAB-SAIUEX) of the Universidad de Extremadura.

AUTHOR CONTRIBUTIONS

N.M.-M. design, performed, and discussed a major part of the experiments; J.M.M. helped in designing the study and organizing and discussing data; A.A.-B. contributed to cell analysis, flow cytometry, and confocal microscopy analysis; D.P.P. and S.T. assisted and helped with metabolomics experiments; J.M.G.-S. helped with *in vitro* assays for Wnt/β-Cat; P.G. helped to perform the analysis of pericentrin; R.M.R. contributed to the design and planning of centrosome experiments; A.M. contributed to the design and planning of Wnt/β-Cat experiments; F.J.G. contributed to the design and planning of metabolomic experiments; P.M.F.-S. designed, discussed, and coordinated the study and wrote the paper.

DECLARATION OF INTERESTS

The authors declare no competing interests.

Received: December 30, 2017
Revised: April 25, 2018
Accepted: May 9, 2018
Published: June 29, 2018

REFERENCES

Antonczak, A.K., Mullee, L.I., Wang, Y., Comartin, D., Inoue, T., Pelletier, L., and Morrison, C.G. (2016). Opposing effects of pericentrin and microcephalin on the pericentriolar material regulate CHK1 activation in the DNA damage response. Oncogene *35*, 2003–2010.

Aylon, Y., and Oren, M. (2011). p53: guardian of ploidy. Mol. Oncol. *5*, 315–323.

Benhamouche, S., Decaens, T., Godard, C., Chambrey, R., Rickman, D.S., Moinard, C., Vasseur-Cognet, M., Kuo, C.J., Kahn, A., Perret, C., et al. (2006). Apc tumor suppressor gene is the "zonation-keeper" of mouse liver. Dev. Cell *10*, 759–770.

Boultwood, J., Yip, B.H., Vuppusetty, C., Pellagatti, A., and Wainscoat, J.S. (2013). Activation of the mTOR pathway by the amino acid (L)-leucine in the 5q- syndrome and other ribosomopathies. Adv. Biol. Regul. *53*, 8–17.

Bunney, T.D., and Katan, M. (2010). Phosphoinositide signalling in cancer: beyond PI3K and PTEN. Nat. Rev. Cancer *10*, 342–352.

Burke, Z.D., Reed, K.R., Phesse, T.J., Sansom, O.J., Clarke, A.R., and Tosh, D. (2009). Liver zonation occurs through a beta-catenin-dependent, c-Myc-independent mechanism. Gastroenterology *136*, 2316–2324.e1-3.

Busca, R., Pouyssegur, J., and Lenormand, P. (2016). ERK1 and ERK2 map kinases: specific roles or functional redundancy? Front. Cell Dev. Biol. *4*, 53.

Cadoret, A., Ovejero, C., Terris, B., Souil, E., Levy, L., Lamers, W.H., Kitajewski, J., Kahn, A., and Perret, C. (2002). New targets of beta-catenin signaling in the liver are involved in the glutamine metabolism. Oncogene *21*, 8293–8301.

Carroll, B., Nelson, G., Rabanal-Ruiz, Y., Kucheryavenko, O., Dunhill-Turner, N.A., Chesterman, C.C., Zahari, Q., Zhang, T., Conduit, S.E., Mitchell, C.A., et al. (2017). Persistent mTORC1 signaling in cell senescence results from defects in amino acid and growth factor sensing. J. Cell Biol. *216*, 1949–1957.

Celton-Morizur, S., Merlen, G., Couton, D., and Desdouets, C. (2010). Polyploidy and liver proliferation: central role of insulin signaling. Cell Cycle *9*, 460–466.

Celton-Morizur, S., Merlen, G., Couton, D., Margall-Ducos, G., and Desdouets, C. (2009). The insulin/Akt pathway controls a specific cell division program that leads to generation of binucleated tetraploid liver cells in rodents. J. Clin. Invest. *119*, 1880–1887.

Chen, T.T., Maevsky, E.I., and Uchitel, M.L. (2015). Maintenance of homeostasis in the aging hypothalamus: the central and peripheral roles of succinate. Front. Endocrinol. (Lausanne) *6*, 7.

Conduit, P.T., Wainman, A., and Raff, J.W. (2015). Centrosome function and assembly in animal cells. Nat. Rev. Mol. Cell Biol. *16*, 611–624.

Conlon, I., and Raff, M. (1999). Size control in animal development. Cell *96*, 235–244.

Contador-Troca, M., Alvarez-Barrientos, A., Barrasa, E., Rico-Leo, E.M., Catalina-Fernandez, I., Menacho-Marquez, M., Bustelo, X.R., Garcia-Borron, J.C., Gomez-Duran, A., Saenz-Santamaria, J., et al. (2013). The dioxin receptor has tumor suppressor activity in melanoma

growth and metastasis. Carcinogenesis *34*, 2683–2693.

Davoli, T., and de Lange, T. (2011). The causes and consequences of polyploidy in normal development and cancer. Annu. Rev. Cell Dev. Biol. *27*, 585–610.

Duncan, A.W., Hanlon Newell, A.E., Bi, W., Finegold, M.J., Olson, S.B., Beaudet, A.L., and Grompe, M. (2012). Aneuploidy as a mechanism for stress-induced liver adaptation. J. Clin. Invest. *122*, 3307–3315.

Duncan, A.W., Hickey, R.D., Paulk, N.K., Culberson, A.J., Olson, S.B., Finegold, M.J., and Grompe, M. (2009). Ploidy reductions in murine fusion-derived hepatocytes. PLoS Genet. *5*, e1000385.

Duncan, A.W., Taylor, M.H., Hickey, R.D., Hanlon Newell, A.E., Lenzi, M.L., Olson, S.B., Finegold, M.J., and Grompe, M. (2010). The ploidy conveyor of mature hepatocytes as a source of genetic variation. Nature *467*, 707–710.

Edgar, B.A., Zielke, N., and Gutierrez, C. (2014). Endocycles: a recurrent evolutionary innovation for post-mitotic cell growth. Nat. Rev. Mol. Cell Biol. *15*, 197–210.

Enan, E., and Matsumura, F. (1996). Identification of c-Src as the integral component of the cytosolic Ah receptor complex, transducing the signal of 2,3,7,8-tetrachlorodibenzo-p-dioxin (TCDD) through the protein phosphorylation pathway. Biochem. Pharmacol. *52*, 1599–1612.

Esser, C., and Rannug, A. (2015). The aryl hydrocarbon receptor in barrier organ physiology, immunology, and toxicology. Pharmacol. Rev. *67*, 259–279.

Fernandez-Salguero, P., Pineau, T., Hilbert, D.M., McPhail, T., Lee, S.S., Kimura, S., Nebert, D.W., Rudikoff, S., Ward, J.M., and Gonzalez, F.J. (1995). Immune system impairment and hepatic fibrosis in mice lacking the dioxin-binding Ah receptor. Science *268*, 722–726.

Fernandez-Salguero, P., Ward, J.M., Sundberg, J.P., and Gonzalez, F.J. (1997). Lesions of aryl-hydrocarbon receptor-deficient mice. Vet. Pathol. *34*, 605–614.

Fox, D.T., and Duronio, R.J. (2013). Endoreplication and polyploidy: insights into development and disease. Development *140*, 3–12.

Ganem, N.J., Storchova, Z., and Pellman, D. (2007). Tetraploidy, aneuploidy and cancer. Curr. Opin. Genet. Dev. *17*, 157–162.

Gao, Z., Bu, Y., Zhang, G., Liu, X., Wang, X., Ding, S., Wang, E., Shi, R., Li, Q., Fu, J., et al. (2016). Effect of TCDD on the fate of epithelial cells isolated from human fetal palatal shelves (hFPECs). Toxicol. Appl. Pharmacol. *305*, 186–193.

Gentric, G., Celton-Morizur, S., and Desdouets, C. (2012). Polyploidy and liver proliferation. Clin. Res. Hepatol. Gastroenterol. *36*, 29–34.

Gentric, G., and Desdouets, C. (2014). Polyploidization in liver tissue. Am. J. Pathol. *184*, 322–331.

Gerbal-Chaloin, S., Dume, A.S., Briolotti, P., Klieber, S., Raulet, E., Duret, C., Fabre, J.M., Ramos, J., Maurel, P., and Daujat-Chavanieu, M. (2014). The WNT/beta-catenin pathway is a transcriptional regulator of CYP2E1, CYP1A2, and aryl hydrocarbon receptor gene expression in primary human hepatocytes. Mol. Pharmacol. *86*, 624–634.

Gerlyng, P., Abyholm, A., Grotmol, T., Erikstein, B., Huitfeldt, H.S., Stokke, T., and Seglen, P.O. (1993). Binucleation and polyploidization patterns in developmental and regenerative rat liver growth. Cell Prolif. *26*, 557–565.

Germain, L., Blouin, M.J., and Marceau, N. (1988). Biliary epithelial and hepatocytic cell lineage relationships in embryonic rat liver as determined by the differential expression of cytokeratins, alpha-fetoprotein, albumin, and cell surface-exposed components. Cancer Res. *48*, 4909–4918.

Guidotti, J.E., Bregerie, O., Robert, A., Debey, P., Brechot, C., and Desdouets, C. (2003). Liver cell polyploidization: a pivotal role for binuclear hepatocytes. J. Biol. Chem. *278*, 19095–19101.

Hannibal, R.L., Chuong, E.B., Rivera-Mulia, J.C., Gilbert, D.M., Valouev, A., and Baker, J.C. (2014). Copy number variation is a fundamental aspect of the placental genome. PLoS Genet. *10*, e1004290.

Jung, Y.S., Qian, Y., and Chen, X. (2010). Examination of the expanding pathways for the regulation of p21 expression and activity. Cell. Signal. *22*, 1003–1012.

Karimian, A., Ahmadi, Y., and Yousefi, B. (2016). Multiple functions of p21 in cell cycle, apoptosis and transcriptional regulation after DNA damage. DNA Repair (Amst) *42*, 63–71.

Ko, C.I., Fan, Y., de Gannes, M., Wang, Q., Xia, Y., and Puga, A. (2016). Repression of the aryl hydrocarbon receptor is required to maintain mitotic progression and prevent loss of pluripotency of embryonic stem cells. Stem Cells *34*, 2825–2839.

Kolluri, S.K., Weiss, C., Koff, A., and Gottlicher, M. (1999). p27(Kip1) induction and inhibition of proliferation by the intracellular Ah receptor in developing thymus and hepatoma cells. Genes Dev. *13*, 1742–1753.

Korzeniewski, N., Wheeler, S., Chatterjee, P., Duensing, A., and Duensing, S. (2010). A novel role of the aryl hydrocarbon receptor (AhR) in centrosome amplification - implications for chemoprevention. Mol. Cancer *9*, 153.

Kurinna, S., Stratton, S.A., Coban, Z., Schumacher, J.M., Grompe, M., Duncan, A.W., and Barton, M.C. (2013). p53 regulates a mitotic transcription program and determines ploidy in normal mouse liver. Hepatology *57*, 2004–2013.

Lahvis, G.P., Lindell, S.L., Thomas, R.S., McCuskey, R.S., Murphy, C., Glover, E., Bentz, M., Southard, J., and Bradfield, C.A. (2000). Portosystemic shunting and persistent fetal vascular structures in aryl hydrocarbon receptor-deficient mice. Proc. Natl. Acad. Sci. USA *97*, 10442–10447.

Laplante, M., and Sabatini, D.M. (2009). mTOR signaling at a glance. J. Cell Sci. *122*, 3589–3594.

Laplante, M., and Sabatini, D.M. (2012). mTOR signaling in growth control and disease. Cell *149*, 274–293.

Lindsey, S., and Papoutsakis, E.T. (2011). The aryl hydrocarbon receptor (AHR) transcription factor regulates megakaryocytic polyploidization. Br. J. Haematol. *152*, 469–484.

Liu, L.L., Long, Z.J., Wang, L.X., Zheng, F.M., Fang, Z.G., Yan, M., Xu, D.F., Chen, J.J., Wang, S.W., Lin, D.J., et al. (2013). Inhibition of mTOR pathway sensitizes acute myeloid leukemia cells to aurora inhibitors by suppression of glycolytic metabolism. Mol. Cancer Res. *11*, 1326–1336.

Ma, D., Yu, H., Lin, D., Sun, Y., Liu, L., Liu, Y., Dai, B., Chen, W., and Cao, J. (2009). S6K1 is involved in polyploidization through its phosphorylation at Thr421/Ser424. J. Cell Physiol. *219*, 31–44.

Macleod, K.F., Sherry, N., Hannon, G., Beach, D., Tokino, T., Kinzler, K., Vogelstein, B., and Jacks, T. (1995). p53-dependent and independent expression of p21 during cell growth, differentiation, and DNA damage. Genes Dev. *9*, 935–944.

Marques, J.M., Olsson, I.A., Ogren, S.O., and Dahlborn, K. (2008). Evaluation of exploration and risk assessment in pre-weaning mice using the novel cage test. Physiol. Behav. *93*, 139–147.

Mathew, L.K., Simonich, M.T., and Tanguay, R.L. (2009). AHR-dependent misregulation of Wnt signaling disrupts tissue regeneration. Biochem. Pharmacol. *77*, 498–507.

Matsubara, T., Tanaka, N., Krausz, K.W., Manna, S.K., Kang, D.W., Anderson, E.R., Luecke, H., Patterson, A.D., Shah, Y.M., and Gonzalez, F.J. (2012). Metabolomics identifies an inflammatory cascade involved in dioxin- and diet-induced steatohepatitis. Cell Metab. *16*, 634–644.

Miettinen, T.P., Pessa, H.K., Caldez, M.J., Fuhrer, T., Diril, M.K., Sauer, U., Kaldis, P., and Bjorklund, M. (2014). Identification of transcriptional and metabolic programs related to mammalian cell size. Curr. Biol. *24*, 598–608.

Mitchell, K.A., Lockhart, C.A., Huang, G., and Elferink, C.J. (2006). Sustained aryl hydrocarbon receptor activity attenuates liver regeneration. Mol. Pharmacol. *70*, 163–170.

Morales-Hernandez, A., Gonzalez-Rico, F.J., Roman, A.C., Rico-Leo, E., Alvarez-Barrientos, A., Sanchez, L., Macia, A., Heras, S.R., Garcia-Perez, J.L., Merino, J.M., et al. (2016). Alu retrotransposons promote differentiation of human carcinoma cells through the aryl hydrocarbon receptor. Nucleic Acids Res. *44*, 4665–4683.

Moreno-Marín, N., Barrasa, E., Morales-Hernández, A., Paniagua, B., Blanco-Fernández, G., Merino, J.M., and Fernández-Salguero, P.M. (2017). Dioxin receptor adjusts liver regeneration after acute toxic injury and protects against liver carcinogenesis. Sci. Rep. *7*, 10420.

Mulero-Navarro, S., and Fernandez-Salguero, P.M. (2016). New trends in aryl hydrocarbon receptor biology. Front. Cell Dev. Biol. *4*, 45.

Nusse, R., and Clevers, H. (2017). Wnt/beta-catenin signaling, disease, and emerging therapeutic modalities. Cell *169*, 985–999.

Pandit, S.K., Westendorp, B., and de Bruin, A. (2013). Physiological significance of polyploidization in mammalian cells. Trends Cell Biol. *23*, 556–566.

Pandit, S.K., Westendorp, B., Nantasanti, S., van Liere, E., Tooten, P.C., Cornelissen, P.W., Toussaint, M.J., Lamers, W.H., and de Bruin, A. (2012). E2F8 is essential for polyploidization in mammalian cells. Nat. Cell Biol. *14*, 1181–1191.

Payne, E.M., Virgilio, M., Narla, A., Sun, H., Levine, M., Paw, B.H., Berliner, N., Look, A.T., Ebert, B.L., and Khanna-Gupta, A. (2012). L-Leucine improves the anemia and developmental defects associated with diamond-blackfan anemia and del(5q) MDS by activating the mTOR pathway. Blood *120*, 2214–2224.

Pohjanvirta, R. (2012). The AH Receptor in Biology and Toxicology, First Edition (John Wiley & Sons).

Prochazkova, J., Kabatkova, M., Bryja, V., Umannova, L., Bernatik, O., Kozubik, A., Machala, M., and Vondracek, J. (2011). The interplay of the aryl hydrocarbon receptor and beta-catenin alters both AhR-dependent transcription and Wnt/beta-catenin signaling in liver progenitors. Toxicol. Sci. *122*, 349–360.

Puga, A., Ma, C., and Marlowe, J.L. (2009). The aryl hydrocarbon receptor cross-talks with multiple signal transduction pathways. Biochem. Pharmacol. *77*, 713–722.

Puga, A., Marlowe, J., Barnes, S., Chang, C.Y., Maier, A., Tan, Z., Kerzee, J.K., Chang, X., Strobeck, M., and Knudsen, E.S. (2002). Role of the aryl hydrocarbon receptor in cell cycle regulation. Toxicology *181-182*, 171–177.

Raff, M.C. (1996). Size control: the regulation of cell numbers in animal development. Cell *86*, 173–175.

Rey-Barroso, J., Alvarez-Barrientos, A., Rico-Leo, E., Contador-Troca, M., Carvajal-Gonzalez, J.M., Echarri, A., Del Pozo, M.A., and Fernandez-Salguero, P.M. (2014). The dioxin receptor modulates caveolin-1 mobilization during directional migration: role of cholesterol. Cell Commun. Signal. *12*, 57.

Rey-Barroso, J., Colo, G.P., Alvarez-Barrientos, A., Redondo-Munoz, J., Carvajal-Gonzalez, J.M., Mulero-Navarro, S., Garcia-Pardo, A., Teixido, J., and Fernandez-Salguero, P.M. (2013). The dioxin receptor controls beta 1 integrin activation in fibroblasts through a Cbp-Csk-Src pathway. Cell. Signal. *25*, 848–859.

Sabbatini, P., and McCormick, F. (1999). Phosphoinositide 3-OH kinase (PI3K) and PKB/Akt delay the onset of p53-mediated, transcriptionally dependent apoptosis. J. Biol. Chem. *274*, 24263–24269.

Saxton, R.A., and Sabatini, D.M. (2017). mTOR signaling in growth, metabolism, and disease. Cell *169*, 361–371.

Schmidt, J.V., and Bradfield, C.A. (1996). Ah receptor signaling pathways. Annu. Rev. Cell Dev. Biol. *12*, 55–89.

Schmidt, J.V., Su, G.H.-T., Reddy, J.K., Simon, M.C., and Bradfield, C.A. (1996). Characterization of a murine Ahr null allele: involvement of the Ah receptor in hepatic growth and development. Proc. Natl. Acad. Sci. USA *93*, 6731–6736.

Schoenfelder, K.P., and Fox, D.T. (2015). The expanding implications of polyploidy. J. Cell Biol. *209*, 485–491.

Shiojiri, N., Lemire, J.M., and Fausto, N. (1991). Cell lineages and oval cell progenitors in rat liver development. Cancer Res. *51*, 2611–2620.

Sigal, S.H., Rajvanshi, P., Gorla, G.R., Sokhi, R.P., Saxena, R., Gebhard, D.R., Jr., Reid, L.M., and Gupta, S. (1999). Partial hepatectomy-induced polyploidy attenuates hepatocyte replication and activates cell aging events. Am. J. Physiol. *276*, G1260–G1272.

Siu, K.T., Rosner, M.R., and Minella, A.C. (2012). An integrated view of cyclin E function and regulation. Cell Cycle *11*, 57–64.

Sturgill, T.W. (2008). MAP kinase: it's been longer than fifteen minutes. Biochem. Biophys. Res. Commun. *371*, 1–4.

Taub, R. (2004). Liver regeneration: from myth to mechanism. Nat. Rev. Mol. Cell Biol. *5*, 836–847.

Ullah, Z., Lee, C.Y., and Depamphilis, M.L. (2009). Cip/Kip cyclin-dependent protein kinase inhibitors and the road to polyploidy. Cell Div. *4*, 10.

Wang, C., Xu, C.X., Krager, S.L., Bottum, K.M., Liao, D.F., and Tischkau, S.A. (2011). Aryl hydrocarbon receptor deficiency enhances insulin sensitivity and reduces PPAR-alpha pathway activity in mice. Environ. Health Perspect. *119*, 1739–1744.

Wang, Q., Kurita, H., Carreira, V., Ko, C.I., Fan, Y., Zhang, X., Biesiada, J., Medvedovic, M., and Puga, A. (2016). Ah receptor activation by dioxin disrupts activin, BMP, and WNT signals during the early differentiation of mouse embryonic stem cells and inhibits cardiomyocyte functions. Toxicol. Sci. *149*, 346–357.

Wang, X., Willenbring, H., Akkari, Y., Torimaru, Y., Foster, M., Al-Dhalimy, M., Lagasse, E., Finegold, M., Olson, S., and Grompe, M. (2003). Cell fusion is the principal source of bone-marrow-derived hepatocytes. Nature *422*, 897–901.

Yamaguchi, A., Tamatani, M., Matsuzaki, H., Namikawa, K., Kiyama, H., Vitek, M.P., Mitsuda, N., and Tohyama, M. (2001). Akt activation protects hippocampal neurons from apoptosis by inhibiting transcriptional activity of p53. J. Biol. Chem. *276*, 5256–5264.

Yu, J.S., and Cui, W. (2016). Proliferation, survival and metabolism: the role of PI3K/AKT/mTOR signalling in pluripotency and cell fate determination. Development *143*, 3050–3060.

Zack, T.I., Schumacher, S.E., Carter, S.L., Cherniack, A.D., Saksena, G., Tabak, B., Lawrence, M.S., Zhsng, C.Z., Wala, J., Mermel, C.H., et al. (2013). Pan-cancer patterns of somatic copy number alteration. Nat. Genet. *45*, 1134–1140.

Zielke, N., Edgar, B.A., and DePamphilis, M.L. (2013). Endoreplication. Cold Spring Harb. Perspect. Biol. *5*, a012948.

Zimmerman, W.C., Sillibourne, J., Rosa, J., and Doxsey, S.J. (2004). Mitosis-specific anchoring of gamma tubulin complexes by pericentrin controls spindle organization and mitotic entry. Mol. Biol. Cell *15*, 3642–3657.

ISCI, Volume *4*

Supplemental Information

Aryl Hydrocarbon Receptor Promotes Liver Polyploidization and Inhibits PI3K, ERK, and Wnt/β-Catenin Signaling

Nuria Moreno-Marín, Jaime M. Merino, Alberto Alvarez-Barrientos, Daxeshkumar P. Patel, Shogo Takahashi, José M. González-Sancho, Pablo Gandolfo, Rosa M. Rios, Alberto Muñoz, Frank J. Gonzalez, and Pedro M. Fernández-Salguero

Supplementary Figure S1

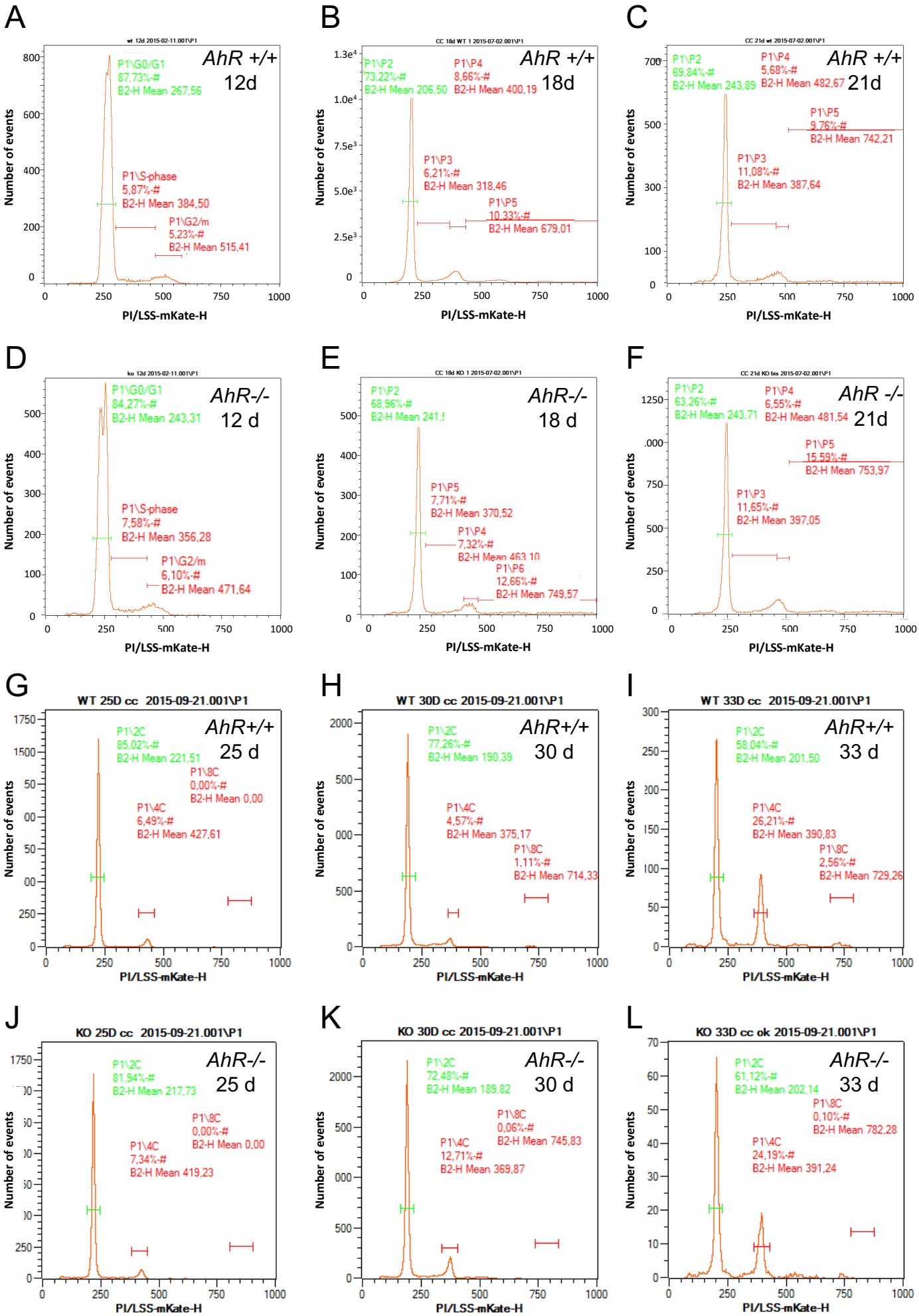

LEGEND FOR SUPPLEMENTARY FIG. S1

Figure S1, related to Fig. 2. Ploidy analysis of preweaning mice. *AhR+/+* and *AhR-/-* preweaning mice between 12 and 33 days of age were analyzed for liver ploidy by flow cytometry. Primary hepatocytes were isolated at the indicated ages, processed for propidium iodide staining and their DNA content analyzed. Mice were at 12 days **(A,D)**, 18 days **(B,E)**, 21 days **(C,F)**, 25 days **(G,J)**, 30 days **(H,K)** and 33 days **(I,L)**. Peaks on the X-axis define DNA content and ploidy status.

Table S1, related to Fig. 2, Fig. 3, Fig. 4, Fig. 5, Fig. 6, Fig. 7, Fig. 8 and Fig. 9

Antibodies used in this study

PROTEIN NAME	REFERENCE	BRAND
AhR	MA1-514	Thermo Scientific
INS-R	Ab131238	Abcam
p85-PI3K	06-497	Millipore-Upstate
PTEN	ab32199	Abcam
pAKT (Ser473)	5048	Cell Signaling
AKT	9272	Cell Signaling
p-GSK3β (Ser9)	5558P	Cell Signaling
GSK3β	12456P	Cell Signaling
pERK1/2 (Thr 202/Tyr204)	9101	Cell Signaling
ERK1/2	9102	Cell Signaling
p53	2524	Cell Signaling
$p21^{Waf1/Cip1}$	2947	Cell Signaling
$p27^{Kip1}$	3686	Cell Signaling
Cyclin E	sc-377100	Santa Cruz Biotechnology
mTOR	ab2732	Abcam
pP70 S6K1 (Tyr389)	9205	Cell Signaling
PCNA	307901	BioLegend
CES3	sc82554	Santa Cruz Biotechnology
Pericentrin	ab4448	Abcam
β-Actin	A2066	Sigma Aldrich
Histone H3	ab1791	Abcam
Cyclin B1	4138	Cell Signaling
Cyclin D1	2978	Cell Signaling
Albumin	4929	Cell Signaling

Table S2, related to Fig. 2, Fig. 6 and Fig. 9

Oligonucleotide primers used in this study

GENE NAME	DIRECTION	PRIMER SEQUENCE (5′-3′)
AhR	forward	AGCCGGTGCAGAAAACAGT
	reverse	AGGCGGTCTAACTCTGTGT
Cyp1a1	forward	ACAGACAGCCTCATTGAGCA
	reverse	GGCTCCACGAGATAGCAGTT
Axin 2	forward	ACTGGGTCGCTTCTCTTGAA
	reverse	CTCCCCACCTTGAATGAAGA
β-Cat	forward	CCCTGAGACCCTACATGAGG
	reverse	TGTCAGCTCAGGAATTGGAC
c-Myc	forward	CCTGACGACGAGACCTTCA
	reverse	TGGTAGGAGGCCAGCTTCT
Cyclin-D	forward	CACAACTTCTCGGCAGTCAA
	reverse	AGTGCGTGCAGAAGGAGATT
Dkk1	forward	GCAGGTGTGGAGCCTAGAAG
	reverse	GCCTCCGATCATCAGACTGT
Lef1	forward	GGGTGTTCTCTGGCCTTGT
	reverse	GCGACTTAGCCGACATCAA
Gapdh	forward	TGAAGCAGGCATCTGAGGG
	reverse	CGAAGGTGGAAGAGTGGGAG
Albumin	forward	TGCATCTAGTGACAAGGTTTGG
	reverse	GACTGGGGCCACTACTTCAA
mTOR	forward	CTCAAGCGATCCAGTTGTCA
	reverse	CAAAGAAGGGCTGAACTTGC

TRANSPARENT METHODS

Mice and treatments

Transgenic *AhR+/+* and *AhR-/-* mice were generated by gene targeting as previously described (Fernandez-Salguero et al., 1995). Preweaning male mice were used at around 25 days of age whereas adult mice were analyzed at 9-10 weeks of age. Previous studies have shown that weaning takes place in mice around 21 days and that polyploidization occurs between 3 and 4 weeks of age (Marques et al., 2008; Pandit et al., 2013; Pandit et al., 2012). Mice were sacrificed at the indicated times and liver tissue was removed and freshly processed for analysis or fixed for immunofluorescence. For metabolomic determinations, serum was obtained from clotted blood. Mice were also perfused through the portal vein of the liver to isolate primary hepatocytes as indicated below. All animal studies have been performed in accordance with the National and European legislation (Spanish Royal Decree RD53/2013 and EU Directive 86/609/CEE as modified by 2003/65/CE, respectively) and in accordance with the Institute of Laboratory Animal Resources (ILAR) for the protection of animals used for research. Experimental protocols were approved by the Bioethics Committee for Animal Experimentation of the University of Extremadura (Registry 109/2014), Junta de Extremadura (EXP-20160506-1) and National Cancer Institute Animal Care and Use Committee. Mice had free access to water and rodent chow.

Antibodies and reagents

The antibodies used in this study are indicated in Table S1. The AhR non-toxic ligand 6-formylindolo[3,2-b]carbazole (FICZ) was obtained from Thermo Scientific and it was used at 10 μM concentration. PI3K inhibitor LY294002, ERK inhibitor PD98059 and Wnt/β-cat inhibitor salynomicin were obtained from MedChem and were dissolved in sterile DMSO.

Reverse transcription and real-time PCR

Total RNA was purified from livers of preweaning and adult mice. Tissues were extracted in a Trizol reagent (Ambion)/chloroform solution, centrifuged and the supernatant precipitated with isopropanol. After centrifugation at 15000 *g* for 30 min at 4ºC, pellets were dissolved in DEPC-treated water and the crude RNA solution further purified using the High Pure RNA Isolation Kit (Roche). Reverse transcription was performed using random priming and iScript Reverse Transcription Super Mix (Bio-Rad). Real-time PCR (qPCR) was performed using SYBR® Select Master Mix (Life Technologies) in a Step One Thermal Cycler (Applied Biosystems) essentially as indicated (Morales-Hernandez et al., 2016; Rico-Leo et al., 2016). *Gapdh* was used to normalize target gene expression (ΔCt) and $2^{-\Delta\Delta Ct}$ to quantify changes in mRNA levels with respect to basal conditions. The oligonucleotide primer sequences used are indicated in Table S2.

SDS-PAGE electrophoresis and Western blotting

SDS-PAGE and Western blotting were performed using total protein liver extracts as described (Rico-Leo et al., 2016). In brief, *AhR*+/+ and *AhR*-/- liver tissues were homogenized in lysis buffer, centrifuged and protein concentration determined in the supernatants using the Coomassie Plus protein assay reagent (Pierce) and bovine serum albumin as standard. Aliquots of 20-30 μg total protein were electrophoresed in 8% SDS-PAGE gels which were transferred to nitrocellulose membranes by electroblotting. Following blocking in TBS-T solution containing 5% non-fat milk, membranes were sequentially incubated with the primary and the secondary antibodies, washed in TBS-T and revealed using the Super-signal luminol substrate (Pierce). Blots were scanned and protein expression quantified in a ChemiDoc XRS+ equipment (Bio-Rad).

Primary hepatocytes isolation by liver perfusion

To obtain primary hepatocyte cultures from mice, a two-step collagenase perfusion protocol was used essentially as described (Tanaka et al., 2015). Some technical modifications were introduced for *AhR-/-* mice in order to optimize perfusion efficiency due to their altered intrahepatic vasculature (Corchero et al., 2004; Lahvis et al., 2000). Mice were anesthetized, the internal organs set aside and the portal vein cannulated. The liver was initially rinsed with 40 ml of Hank's buffered salt solution (HBSS) containing 1 mM EDTA but without calcium and magnesium (Gibco) to remove blood. To drain the liver, the inferior vena cava was cut at the beginning of the process. Perfusion was done by passing 50 ml of a HBSS solution containing 0.6 mg/ml collagenases I and II (Gibco) and $CaCl_2$ through the cannulated portal vein. The liver was then removed, placed in a sterile tissue culture dish and the gallbladder carefully excised. Liver cells were gently detached, filtered through a 70 μm mesh cell strainer (Falcon) and centrifuged at 400 g for 3 minutes at 4°C. Primary hepatocytes were purified through a Percoll gradient (GE Healthcare), washed with PBS, stained with trypan blue to determine the number of dead cells and seeded in collagen-treated tissue culture plates at the appropriate cell density in DMEM-F12 medium (Lonza) supplemented with 10% FBS, 2 mM glutamine, 100 U/ml penicillin and 100 μg/ml streptomycin. For some experiments, hepatocyte growth factor (HGF) and epidermal growth factor (EGF) were added to the medium.

***In vitro* and *in vivo* treatment with pharmacological inhibitors**

Primary hepatocyte cultures isolated from *AhR-/-* mice were seeded at a confluence of $1x10^6$ cells/well in 6-well plates and allowed to attach overnight. Cultures were then treated for 48 h with PI3K inhibitor LY294002 (25 and 50 μM), ERK inhibitor PD98059 (5 and 10 μM) and Wnt/β-cat inhibitor salynomicin (2,5 and 5 μM). Control cultures received the same concentration of the solvent DMSO. For *in vivo* inhibition of signaling

pathways, *AhR-/-* mice were treated for 7 days with a mix of 30 mg/kg LY294002 + 10 mg/kg PD98059 by i.p. injection plus 8 mg/kg salynomicin in drinking water. Control mice were injected with the same volume of DMSO. At the end of treatment, mice were sacrificed and their liver ploidy status analyzed by flow cytometry.

Ploidy analysis

Primary hepatocytes from *AhR+/+* and *AhR-/-* mice were fixed with 70% ethanol for 30 min at -20ºC and incubated with 10 μg/ml RNAse for 30 min at 37ºC. DNA content per cell was determined in a MACSQuant VYB (Miltenyi Biotech) after staining the cells with 50 μg/ml propidium iodide for 15 min at room temperature in the dark. Only signals from single cells were considered and at least 10.000 events were analyzed per sample. To quantify the number of binucleated cells, liver sections from preweaning and adult mice of each genotype were stained with DAPI and the number of hepatocytes containing two-nuclei counted using confocal fluorescence microscopy. Data are shown as the fraction of binucleated hepatocytes with respect to the total number of hepatocytes per field.

Wnt/β-Cat luciferase reporter assay

AhR+/+ and *AhR-/-* primary hepatocytes were seeded at a density of $4x10^5$ cells/well on Collagen-I pre-treated 12-well plates (Becton-Dickinson). After overnight incubation, cells were co-transfected with 1 μg TOPflash (TCF-binding sites-containing vector) or FOPflash (TCF-mutant binding sites-containing vector) expression plasmids (Millipore) and 0.4 μg pRL-TK (*Renilla* TK-luciferase vector, Promega) using Lipofectamine 3000 (Life Technologies). Luciferase activities were measured in a Varioskan Flash 96 Microplate Luminometer (Thermo Scientific) and, for each experimental condition, firefly luciferase (e.g. from TOPflash- or FOPflash-transfected primary hepatocytes) was normalized by *Renilla* luciferase. β-Cat-driven transcription was calculated as the

TOP/FOP ratio following normalization. In some experiments, primary hepatocytes were treated with Wnt3a-enriched medium (1:4 dilution) obtained from L1-Wnt3a cells grown in DMEM medium supplemented with 10% FBS, 2 mM glutamine, 100 U/ml penicillin and 100 μg/ml streptomycin. Parallel cultures received medium from control L1 cells.

IRS-2 activation assay

Activation of the Insulin receptor signaling intermediate IRS-2 was determined by using the PathScan Phospho-IRS-2 ELISA Kit (Thermo Scientific). Briefly, sections of 50 mg liver tissue were homogenized with a MagNA Lyser equipment (Roche) in cell lysis buffer. Homogenates were then sonicated during 3 min on ice and protein concentration determined as indicated above. Aliquots of 100 μg and 250 μg total liver protein were added to the 96-well ELISA plate and the levels of pIRS-2 determined following the protocol provided by the manufacturer. Mice injected i.p. with 1 unit insulin were used as positive controls.

Immunoprecipitation

AhR+/+ and *AhR*-/- liver tissues were homogenized with a MagNA Lyser equipment (Roche) in lysis buffer (50 mM Tris pH 7.5, 150 mM NaCl, 1% NaCl, 1% NP40, 10% glycerol, 2 mM EDTA, 1% PMSF and Halt protease inhibitor cocktail (Thermo Scientific)). Homogenates were centrifuged at 10000 g for 5 min at 4°C and protein concentration was quantified using the BCA protein assay kit (Beyotime Biotech). Aliquots of 2 mg liver protein were immunoprecipitated using Dynabeads Protein G (Life Technologies) and antibodies against AhR and pAKT essentially as described (Rey-Barroso et al., 2014; Rico-Leo et al., 2013).

Hematoxylin/eosin staining of liver sections

Livers from *AhR*+/+ and *AhR*-/- mice were fixed overnight at room temperature in buffered formalin and included in paraffin. Sections of 3 μm were deparaffinated in xylol

and re-hydrated to phosphate buffered saline (PBS). Sections were incubated for 3 min with hematoxylin, washed with tap water and stained with eosin for 1 min. Sections were de-hydrated, mounted and observed in a NIKON TE2000U microscope using 4x (0.10 numeric aperture) and 10x (0.25 numeric aperture) objectives.

Immunofluorescence and confocal microscopy

Liver sections prepared as indicated above were incubated for 1 h at room temperature in PBS containing 0.25% Triton X-100 (PBS-T), 0.2% gelatin and 3% BSA to block unspecific epitopes. Sections were incubated overnight at 4ºC with anti-β-Cat primary antibody diluted in PBS-T containing 0.2% gelatin. After washing in the same solution, tissues were incubated for 1 h at room temperature with an Alexa-633-labeled secondary antibody. After further washing, sections were dehydrated, mounted on Mowiol and visualized using an Olympus FV1000 confocal microscope (Olympus). For some experiments, 10 μm liver sections were processed as indicated above and incubated with anti-PCNA primary antibody and Alexa-488 secondary antibody. Sections were analyzed with the same confocal microscope equipped with a multiphoton laser. Objectives used were: 10x (0.40 numeric aperture) and 20x (0.70 numeric aperture). Fluorescence analysis was done using the FV10 software (Olympus). DAPI was used to stain cell nuclei.

Metabolomic analyses by GC-MS

Blood was collected from *AhR*+/+ and *AhR*-/- group mice and serum prepared using Serum Separator Tubes (Becton-Dickinson) as indicated by the manufacturer. GC-MS analysis was performed with an Agilent 6890N gas chromatograph coupled to an Agilent 5973 mass-selective detector (MSD) as previously described (Patel et al., 2017) for the tricarboxylic cycle intermediates, amino acid (L-Leucine, L-Glutamine) and dicarboxylic acid (Azelaic acid) analysis. Additionally, m/z (Qualifier ions 1 -Q1, Qualifier ions 2 -

Q2) for L-leuicine 200 (274,302), and Azelaic acid 317 (359,201) at retention time 13.3 min and 18.8 min in sequence were selected for single ion monitoring by GC-MS. Data Processing were conducted with agilent mass hunter work station software.

Metabolomics profiling with UPLC-ESI-QTOFMS

UPLC-ESI-QTOFMS analysis was performed as previously reported (Matsubara et al., 2012). Samples were introduced into the mass spectrometer Q-TOF Premier (Waters Corporation) operating in either negative or positive electrospray ionization modes. Data processing and multivariate data analysis were conducted as previously reported (Matsubara et al., 2012). A PCA, PLS-DA and contribution analyses were performed using SIMCA-P+12 (Umetrics).

Statistical analyses

Quantitative data are shown as mean ± SD. Comparisons between experimental conditions was done using GraphPad Prism 6.0 software (GraphPad). The student´s t test was used to analyze differences between two experimental groups and ANOVA for the analyses of three or more groups. The Mann-Whitney non-parametric statistical method was used to compare rank variations between independent groups.

SUPPLEMENTAL REFERENCES

Corchero, J., Martin-Partido, G., Dallas, S.L., and Fernandez-Salguero, P.M. (2004). Liver portal fibrosis in dioxin receptor-null mice that overexpress the latent transforming growth factor-beta-binding protein-1. Int J Exp Pathol 85, 295-302.

Lahvis, G.P., Lindell, S.L., Thomas, R.S., McCuskey, R.S., Murphy, C., Glover, E., Bentz, M., Southard, J., and Bradfield, C.A. (2000). Portosystemic shunting and persistent fetal vascular structures in aryl hydrocarbon receptor-deficient mice. Proc Natl Acad Sci USA 97, 10442-10447.

Marques, J.M., Olsson, I.A., Ogren, S.O., and Dahlborn, K. (2008). Evaluation of exploration and risk assessment in pre-weaning mice using the novel cage test. Physiol Behav 93, 139-147.

Matsubara, T., Tanaka, N., Krausz, K.W., Manna, S.K., Kang, D.W., Anderson, E.R., Luecke, H., Patterson, A.D., Shah, Y.M., and Gonzalez, F.J. (2012). Metabolomics identifies an inflammatory cascade involved in dioxin- and diet-induced steatohepatitis. Cell Metab 16, 634-644.

Morales-Hernandez, A., Gonzalez-Rico, F.J., Roman, A.C., Rico-Leo, E., Alvarez-Barrientos, A., Sanchez, L., Macia, A., Heras, S.R., Garcia-Perez, J.L., Merino, J.M*., et al.* (2016). Alu retrotransposons promote differentiation of human carcinoma cells through the aryl hydrocarbon receptor. Nucleic Acids Res 44, 4665-4683.

Pandit, S.K., Westendorp, B., and de Bruin, A. (2013). Physiological significance of polyploidization in mammalian cells. Trends Cell Biol 23, 556-566.

Pandit, S.K., Westendorp, B., Nantasanti, S., van Liere, E., Tooten, P.C., Cornelissen, P.W., Toussaint, M.J., Lamers, W.H., and de Bruin, A. (2012). E2F8 is essential for polyploidization in mammalian cells. Nat Cell Biol 14, 1181-1191.

Patel, D.P., Krausz, K.W., Xie, C., Beyoglu, D., Gonzalez, F.J., and Idle, J.R. (2017). Metabolic profiling by gas chromatography-mass spectrometry of energy metabolism in high-fat diet-fed obese mice. PLoS One 12, e0177953.

Rey-Barroso, J., Alvarez-Barrientos, A., Rico-Leo, E., Contador-Troca, M., Carvajal-Gonzalez, J.M., Echarri, A., Del Pozo, M.A., and Fernandez-Salguero, P.M. (2014). The Dioxin receptor modulates Caveolin-1 mobilization during directional migration: role of cholesterol. Cell communication and signaling : CCS 12, 57.

Rico-Leo, E.M., Moreno-Marin, N., Gonzalez-Rico, F.J., Barrasa, E., Ortega-Ferrusola, C., Martin-Munoz, P., Sanchez-Guardado, L.O., Llano, E., Alvarez-Barrientos, A., Infante-Campos, A., *et al.* (2016). piRNA-associated proteins and retrotransposons are differentially expressed in murine testis and ovary of aryl hydrocarbon receptor deficient mice. Open Biol 6:160186.

Tanaka, N., Takahashi, S., Zhang, Y., Krausz, K.W., Smith, P.B., Patterson, A.D., and Gonzalez, F.J. (2015). Role of fibroblast growth factor 21 in the early stage of NASH induced by methionine- and choline-deficient diet. Biochim Biophys Acta 1852, 1242-1252.